Freie Universität Berlin

Fachbereich Geowissenschaften

Institut für Geologische Wissenschaften

Quartz grain weathering in a periglacial environment:

Indications from SEM and TEM studies using single grain features

Masterarbeit

zur Erlangung des akademischen Grades

Master of Science

Vorgelegt von: Franziska Frütsch

Gutachter: PD Dr. Ekkehard Scheuber (Freie Universität Berlin)

PD Dr. Bernhard Diekmann (Alfred-Wegener-Institut für Polar- und Meeresforschung Potsdam)

Juli 2011

Selbstständigkeitserklärung

Hiermit versichere ich, dass ich die vorliegende Arbeit selbstständig und nur unter Verwendung der in der Arbeit verzeichneten Literatur und Hilfsmittel angefertigt habe.

Berlin, Juli 2011 Franziska Frütsch

CONTENTS

ABSTRACT

The study investigates the quartz grain breakup behavior under cryogenic conditions. It has been introduced by some scientists thus its applicability as a proxy for paleoclimate reconstruction is still in debate. Eight samples from permafrost and non-permafrost regions were tested for quartz grain fragmentation under laboratory conditions by applying >100 freeze/thaw cycles. The in-situ weathering condition have been simulated on the basis of Konishchev's (1982) pioneering work thereby using scanning-electron microscopy (SEM) for identifying grain shape and surface features. The optical microscopy (OM) and transmission electron microscopy (TEM) were used for identifying internal quartz impurities, and Laser particle sizing (LS) for grain size measurement to substantiate the results. Quartz grain fragmentation into silt sized particles after the cryogenic experiment is associated with frequently observed micro cracks and mineral impurities related to common seen inclusions. These micro cracks and impurities may act as weakening zones of the mineral grains when thermal stress, ice growth in fissures and water volume changes. These are effective forces of freeze-thaw weathering dynamics. The enrichment of quartz in the smaller grain size fraction after the cryogenic experiment suggests that the sensitivity of quartz grain breakup under cryogenic condition can be used as a proxy for cold-climate weathering. This is wide spread which occurs in Alpine as well as in polar areas, since this behavior contrasts the common quartz resistance to weathering in lower latitudes. It may allow for identifying permafrost episodes in the geologic past when studying paleoclimate and paleoenvironmental archives. Its validity is discussed in connection with the El'gygytgyn Crater Lake site in Arctic Siberia, where from Late Cenozoic sediment archives have become available only recently.

KURZFASSUNG

Die Studie untersucht die Quarzkornzersplitterung unter kryogenen Bedingungen. Dieses zerbrechen der Quarze wurde von einigen Wissenschaftlern untersucht aber seine Anwendbarkeit als Proxy für Paläoklimarekonstruktion wird noch debattiert. Acht Proben aus Permafrost und Nicht-Permafrost Gebieten wurden verwendet um das

Quarzkornauseinanderbrechen unter Laborbedingungen bei > 100 Frier/Tauwechseln (F/T) nachzuvollziehen. Die in-situ Verwitterungsbedingungen wurden auf Basis von Konishchev's (1982) Pionierarbeit durchgeführt. Dabei wurden das Rasterelektronenmikroskop (REM) zur Oberflächen- und Formanalyse sowie die optische Mikroskopie (OM) als auch das Transmissionselektronenmikroskop (TEM) für die mikrostrukturellen Schwächezonen im Quarz verwendet. Als Nachweis für das Quarzkornzerbrechen wurde die Korngrößenbestimmung mit Hilfe des Laser particle sizing (LS) durchgeführt. Das beobachtete Quarzkornzerbrechen nach dem kryogenen Experiment ist assoziiert mit den häufig beobachteten Mikrobrüchen und den Mikroverunreinigungen durch Einschlüssen. Diese Mikrobrüche und Verunreinigungen können bei thermalem Stress, Eissegregation und Volumenänderungen als Schwächezonen im Quarz fungieren, welche unter kryogenen Bedingungen (F/T) effektive Kräfte sind. Die Anreicherung von Quarz in der kleineren Fraktion nach dem Experiment legt nahe, dass durch die Sensibilität von Quarz bei kryogenen Bedingungen es als Proxy für cold-climate Verwitterung verwendet werden kann. Diese cold-climate Verwitterungsbedingungen sind weitverbreitet und erstrecken sich im Alpinen, als auch in polaren Gebieten (Permafrostgebiete), welche durch das typisch schnellere verwittern des Quarzes in den niedrigen Breitengraden gekennzeichnet ist. Es könnte uns die Möglichkeit geben Permafrost Episoden in Paläoklima- und Paläoumweltarchiven zu identifizieren. Seine Aussagekraft als Proxy ist in Verbindung mit dem El'gygytgyn See im arktischen Sibirien diskutiert wo kürzlich Spätkänozoische Sedimentarchive erschlossen wurden.

AIMS AND OBJECTIVES

The understanding of rock weathering dynamics with regard to changing climate conditions is of principal interest to geosciences for improving past climate reconstruction. This Master's thesis focuses on studying cold-climate weathering effects on rock disintegration with specific attention to the physical behavior of quartz grains. Several studies have observed unusually high amounts of silt in Quaternary deposits at higher latitudes when compared with lower latitudes (e.g. Konishchev, 1982; Vasiliyev, 1994). Silt production in permafrost areas is commonly associated with quartz grain enrichment due to frost induced quartz grain disintegration processes (Konishchev and Rogov, 1993). This indicates that quartz grains seem to breakup easier in a permafrost environment under periglacial conditions than elsewhere. But what are the physical mechanisms of this breakup? In order to improve understanding of quartz breakup under permafrost conditions an experimental set-up was established that allowed observation of the fracturing of quartz grains following repeated freeze/thaw (F/T) cycles. Single quartz grain studies were undertaken on defining quartz grain morphology features using SEM (scanning electron microscopy) and TEM (transmission electron microscopy) techniques as well as OM (optical microscopy) with the aims of better understanding the physical mechanisms of quartz fracturing. The aim of this thesis is to better understand the physical mechanism of quartz fracturing under cryogenic weathering conditions. To be able to use quartz grains in this way would be important because the quartz grain signatures potentially could be used as a proxy in paleoclimate research for reconstructing periglacial conditions in sedimentary environments.

1 INTRODUCTION

1.1 PERIGLACIAL ENVIRONMENT

The term periglacial includes a range of cold (freezing point), non-glacial processes. The periglacial environments are characterized by frost action and the seasonal presence of snow cover. Periglacial regions are most prominent in the Arctic area (Figure 1) but also in the Antarctic. The tree line is among others an ecological boundary that is commonly associated with the delimitation of the periglacial environment (http://www.uio.no/studier/emner/matnat/geofag/GEG2130/h08/undervisningsmateriale/GEG2130%20Periglacial%20geomorphology.pdf (12.01.2011)).

Therefore, based on the treeline boundaries, the global extent of periglacial zones can be classified into five zones: (1) High Arctic climates; (2) Continental climates; (3) Alpine climates; (4) Qinghai-Xizang (Tibet) plateau and (5) Climates of low annual temperature ranges (French, 2007, p. 33-34).

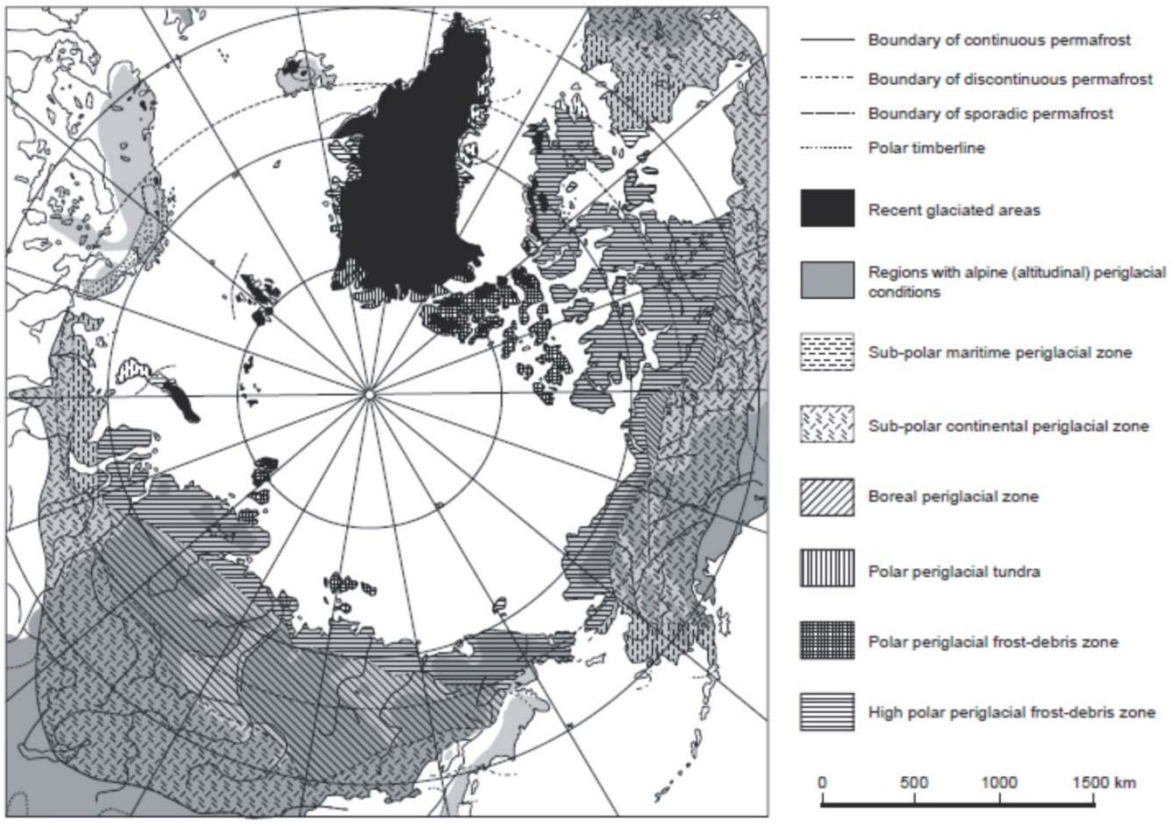

Figure 1: The regional extend of periglacial areas in the northern hemisphere (Karte and Liedke, 1981).

1.2 Definition and distribution of Permafrost

Permafrost is a widespread phenomenon which covers over 20% of the Earth‘s land area and exists anywhere where the general annual air temperature is at or less than the freezing point of water (French, 2007, p.83). Geographically, permafrost commonly occurs in high latitudes but also in mountain areas (alpine permafrost) when air temperatures are constantly below or at the freezing point. Further, permafrost occurs up to latitude 84°N in northern Greenland, and as far south as latitude 26°N in the Himalayas (Figure 1.2). It exists in 23-25% of exposed land in the Northern Hemisphere. Hence, Russia possesses the largest area of permafrost landscape; Canada and China have the second and third largest areas of permafrost (French, 2007, p.94).

The permafrost conditions are influenced by the characteristics of ground material (e.g. thermal conductivity and diffusivity), water chemistry and existence, vegetation, snow cover, topography and air temperature. Based on spatial extent permafrost is divided in two main types: *continuous* and *discontinuous* permafrost.

Continuous and discontinuous permafrost

Continuous permafrost (CPZ) is marked by frozen ground, which has been experiencing at least *two years of* continuous temperatures at or below freezing point of water (Mueller, 1943). Parts of the ground can be still unfrozen depending on their chemical composition (e.g. sodium) because permafrost with saline soil moisture might not be frozen at air temperatures from 0°C and colder. Also in front of glaciers permafrost may not be continuous because snow might function as an insulating blanket and prevent the ground from freezing during winter.

Discontinuous permafrost occurs at areas with mean annual temperatures slightly below 0°C, usually in higher latitudes in areas where strong seasonal fluctuation is present marked by warm summers and cold winters (e.g. Northern Scandinavia) and forms only in sheltered spots. In general, permafrost will remain discontinuous when the mean annual soil surface temperature is between -5 and 0°C (French, 2007, p. 98). Discontinuous permafrost covers between 50 and 90 percent of the landscape with mean annual temperature between -2 and

-4°C and *sporadic permafrost* (SPZ) marked by cover area less than 50 percent of the landscape and a mean annual temperature between 0 and -2°C (French, 2007, p. 94-97).

The line of continuous permafrost describes the geographical extension of the permafrost which is well mapped in the Northern Hemisphere. This line forms at the northerly limit where permafrost does still thaw or no permafrost exist. From this latitude north the landscape is covered by permafrost or glacial ice (French, 2007, p. 12).

THE ACTIVE LAYER

Permafrost has an active layer, which thaws during summer and refreezes in winter. The thickness of the active layer varies with the geographical position as well as by several control mechanism such as air/ground temperature, snow cover, vegetation and soil (Figure 2). In Polar Regions, the active layer becomes the thinnest (≤ 15cm) compared to sub -arctic regions where its thickness increases (≥ 1m). If the warm phases continue, the active layer will progressively thicken in years (French, 2007, p. 112-113).

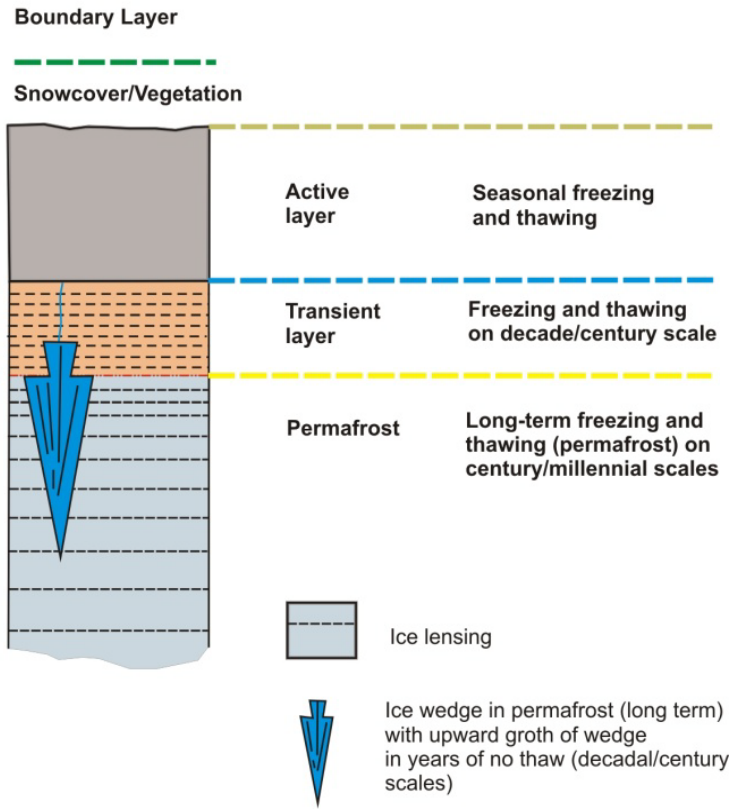

Figure 2: Schematic illustration of the three-layer model (active layer-transient layer-permafrost). This sketch is modified from French (2007), p. 112.

The transient layer marks the long-term position of the contact between the active layer and the upper part of the permafrost (French, 2007, p. 111-113). The thickness of the transient

layer varies in response to summer warming. This transient layer consists mostly of ice which could lead by thawing to slope instability and rapid mass movement (active-layer-detachment-failure) also known as solifluction (French, 2007, p. 111-113).

1.3 COLD-CLIMATE WEATHERING

Cold-climate weathering is a complex term for *cryogenic weathering* and *frost action* which is explained in detail in the following sections.

FROST ACTION

Frost action includes distinctive processes generated by freezing and thawing effects in soils, rock and other material. The influence of these effects varies by soil specific characteristics of heat conductivity and the presence of moisture content. There are basically two processes occurring due to frost action in soil: 1. frost heave and 2. thawing weakening and settlement due to freeze-thaw events (French, 2007, p. 49). The most important process in regard to this Master's Thesis is thawing weakening and settlement and its effects on soil under freeze-thaw events.

FREEZING AND THAWING

Freezing and thawing cycles are of particular importance for the formation of pore and segregated ice with respect to frost wedging and rock shattering (Douglas et al., 1983). It is known that the volume of pure water increases by approximately 9% (Bridgman, 1912) when it turns into ice below the freezing point. In permafrost landscapes this volume increase becomes obvious for example as frost heave in the hummocky tundra. Further, the capillarity in soil is an important factor for the physical processes in a frost environment. Molecular forces in soil exist between phases (freezing and thawing) when the soil is confined (e.g. delimited zone) (Williams & Smith 1989). The capillarity between soil particles increases as the soil particles become smaller. Soil capillarity and the soil related adsorption characteristics are important factors for the rate and intensity of cryogenic weathering.

Numerous studies have been conducted in freezing and thawing cycles (see chapter cryogenic weathering effects-experimental studies) to interpret the results for basic climate

understanding and reconstruction. For seasonal regime, the measurement of the ground temperature is well suited, especially in periglacial landscapes, to identify cold and warm phases. As illustrated in figure 3, the amount of freeze-thaw days varies depending on geographic position.

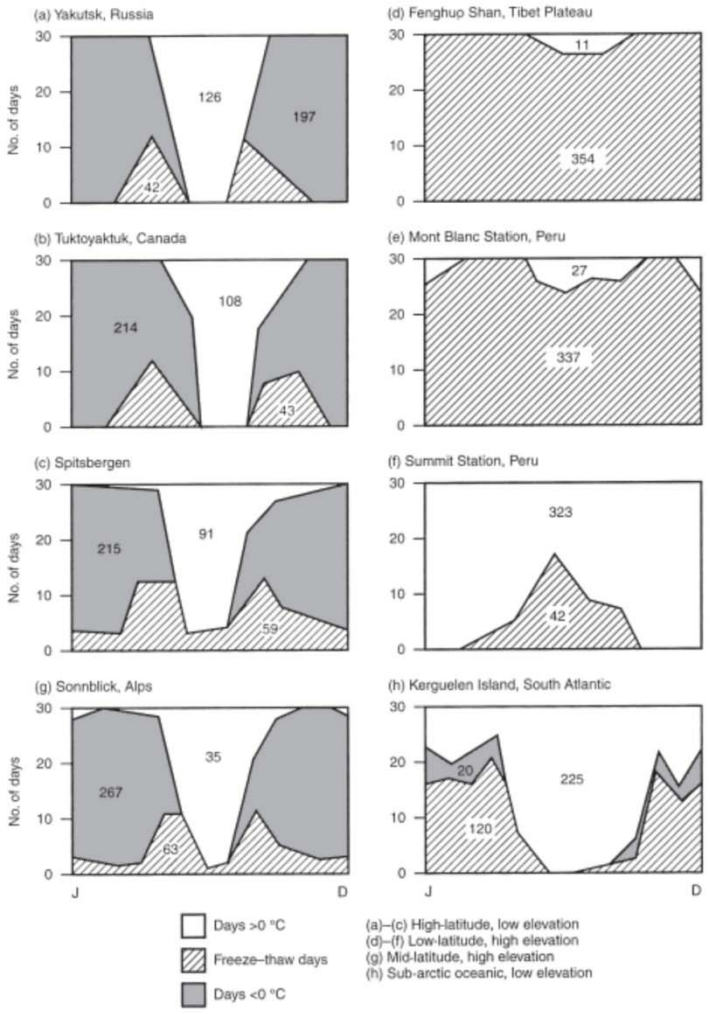

Figure 3: Freezing and thawing conditions in various periglacial environments of the world: (a) Yakutsk, Siberia, Russia; (b) Tuktoyaktuk, Mackenzie Delta, Canada; (c) Green Harbor, Spitzbergen; (d) Fenghuo Shan, Quinghai-Xizang (Tibet) plateau, China; (e) Mont Blanc Station, El Misti, South Peru; (f) Summit Station, El Misti, South Peru; (g) Sonnenblick, Austria; (h) Kerguelen Island, Southern (Indian) Ocean (see sources in French, 2007 p. 37)

Hence, the resolution of cold and warm phases is more problematic and depends on several factors (e.g. soil characteristic, water availability and chemistry, air vs. ground temperature).

CRYOGENIC WEATHERING

Cryogenic weathering is related to a combination of mechanic-chemical processes which leads to in-situ disintegrations of rock under cold-climate conditions. Studies in the former Soviet Union conclude that the production of silt particles of grain sizes between 0.005 mm

and 0.01 mm in diameter of quartz, feldspar as well as of amphibole and pyroxene especially in Siberia are due to frost weathering (Konishchev, 1982).

CRYOGENIC WEATHERING EFFECTS – EXPERIMENTAL STUDIES

Extensive studies of cryogenic weathering have been performed by Konishchev (1982) where he focused on the mechanical behavior of soils especially of quartz, feldspar and heavy minerals, in loess regions in the former Soviet Union. A cryogenic experiment has been performed by Konishchev (1982) to reconstruct the condition for frost weathering. During frost weathering a significant increase in smaller quartz grain sizes (0.05-0.01 mm) has been observed that correspond to field observations. In addition, Konishchev and Rogov (1993) imply that frost weathering can only take place when unfrozen water is present. In periglacial environment, permafrost soils thaw and freeze annually, but only strongly localized in the active layer. Due to the presence of water which occurs as an unfrozen film on the surface of particles, particles (e.g. terrigene sediments) absorbed the water and extent during the transition from water to ice. The intensity of weathering not only depends on the availability of water but also of the thickness and property of the water film. Among other studies Hall et al. (2004) for example focused on rock disintegration in northern Canada.

2 STUDY AREA

In the framework of this thesis, the Lake El'gygytgyn has been chosen as a representative area of cold-climate weathering effects on soil due to the availability of a paleo-environmental archive reaching back to about 3.6 Ma (Melles, et al., 2007). As reference data, four additional sample regions from periglacial (Lena Delta) and non-periglacial (Ayers Rock-Australia, Death Valley- USA, dune sands- North Algeria) areas are used to compare the results from Lake El'gygytgyn.

2.1 SETTING OF LAKE EL´GYGYTGYN

Lake El'gygytgyn is located in central Chukotka, northeast of Siberia (67° 30' N, 172° 5' O, and 492 m a.s.l. (meter above sea level)). Lake El'gygytgyn is located within the northwestern part of the Anadyr-mountain range, consisting of volcanic bedrock (mainly ignimbrites, andesites, rhyolites and trachyrhyolites) which are of Late Cretaceous age (e.g. Masaitis, 1999, Asikainen, et al. 2007) (Figure 4).

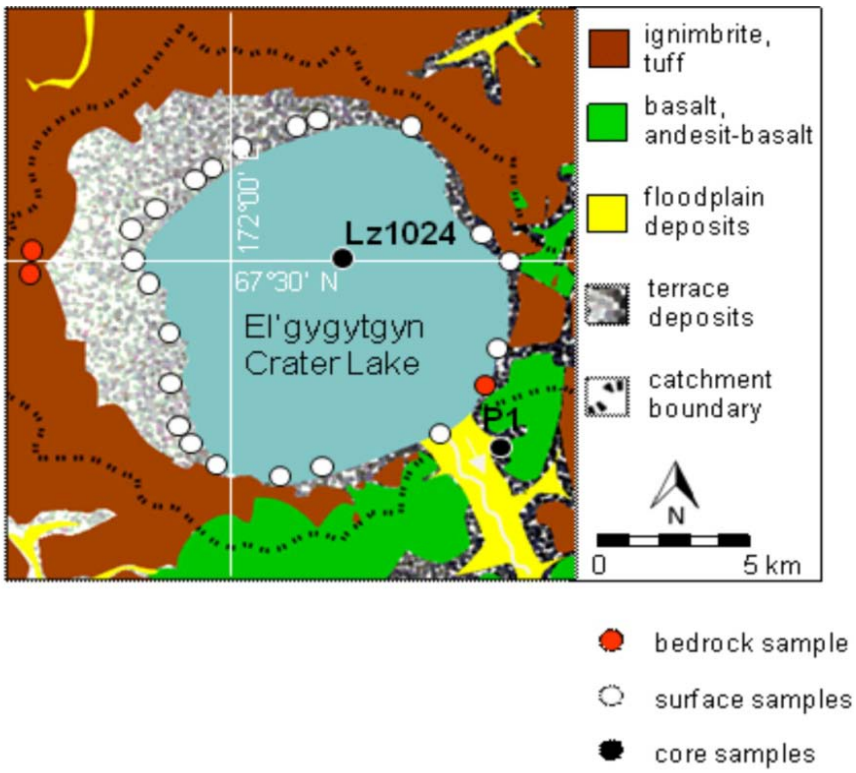

Figure 4: Geological map of Lake El'gygytgyn (modified from Belyi & Chereshnev, 1993; Layer, 2000).

The lake itself has been formed after a meteorite impact, which occurred 3.6 Ma ago generating a crater roughly 18 km in diameter (Layer, 2000). The depression of the impact was filled with water and since then accumulated over 360 m of sediment (Niessen, et al. 2007). These sediments are overlying a brecciated crater floor with an ill-defined central dome (Niessen, et al. 2007).The lake has roughly a circular shape with a diameter of approximately 12 km (Belyi, 1982; Belyi and Chereshnev, 1993; Belyi, et al., 1994) and a maximum water depth of about 175 m. The fresh water input comes from about 50 small streams entering El'gygytgyn Lake at 492 m a.s.l. from a catchment that extends to the crater rim up to 935 m a.s.l. The only drainage of the lake takes place at the southeastern shore into the Enmyvaan River. The area of the Lake El'gygytgyn has never been glaciated (Glushkova, 2001) and the sedimentary fill into the basin likely accumulated continuously. Therefore it is assumed that the lake sediments consist of a complete sedimentary record from about 3.6 Ma to present (Brigham-Grette, et al., 2007).

Climatic data from 2002 show that the mean annual air temperature at the Lake El'gygytgyn was about -10.3°C, with extreme variations from -40°C in winter to +26°C during summer time (Nolan and Brigham-Grette, 2007).

2.2 ADDITIONAL SAMPLES

For the validity of the results, sample material from five different areas of the world has been used to determine the effects of freeze-thaw cycles on terrigeneous sediments. The samples have been obtained in the following areas and represent surface material (also see Table 1).

Samples from North Algeria (*dune sands*) and the United States (*Death Valley*) were kindly provided by Prof. Dr. Christoph Heubeck. The Algerian sample have been obtained in the North Algerian desert and represent sand dunes deposits with strong temperature variations between day and night (~2 – 35°C). The sample from Death Valley (USA) was taken in an arid area with occasional frost events during winter time. The Death Valley is situated in a large basin with a complex geology of active strike-slip and normal faults marked by strong temperature fluctuations. The sample from Ayers Rock - Australia has been collected from

Dr. Georg Schwamborn in 2002. Around Ayers Rock the climate is very dry during summer time and considerable rainfall occurring during winter (~320 mm/a) with high temperature fluctuations of 3.4 during winter time and 37.5 °C during summer time (http://www.bom.gov.au/climate/averages/tables/cw_015527.shtml (07.04.2011)).

Samples from the Lena Delta were taken during two field campaigns performed in 2002 (Dr. Lutz Schirrmeister) and 1998 (Dr. Georg Schwamborn). Both sample areas are situated in a fluvial environment in a continuous permafrost region. Samples from Lake El'gygytgyn in NE Russia have been obtained in two locations: (1) 50 stream sediment samples taken in the creek mouth lobes at the shoreline of the lake. (2) 10 samples of accumulated terrace material taken from the paleo lake rims. The area of these two samples is located in a permafrost region with annual freezing and thawing events.

Table 1: Overview of collected samples used for the cryogenic experiment.

	Kind of sample	**Number of samples used for this cryogenic experiment**	**Collection type**
North Algeria - Dune sands	loose sediments	1	surface sample
USA - Death Valley	loose sediments	1	surface sample
Australia - Ayers Rock	loose sediments	1	surface sample
Lena Delta 1998	loose sediments	1	surface sample
Lena Delta 2002	loose sediments	1	surface sample
Lake El'gygytgyn beach terrace	loose sediments	2	surface sample
Lake El'gygytgyn stream fill	loose sediments	1	surface sample

3 MATERIAL AND METHODS

The cryogenic experiment is based on the former investigations of Konishchev (1982) that revealed different grain disintegration behavior under cryogenic conditions. It was established experimentally that grain sizes of quartz, amphiboles, and pyroxenes are limited for cryogenic disintegration from 0.05 to 0.01 mm. Feldspar however shows only limitations from 0.1 to 0.05 mm under cryogenic conditions. But what are the trigger mechanisms for quartz to breakup easier than feldspar? To analyze these mechanisms a series of freeze-thaw cycles have been conducted to reconstruct the effects of cryogenic weathering. In addition, a range of methods (grain size measurements, TEM, SEM and optical microscopy) have been used to analyze and quantify changes in grain sizes and grain micromorphology (see Table 2).

Table 2: Analytical methods used for the cryogenic experiment

Sample/Method	TEM	OM	Laser Coulter	SEM
Ayers Rock	x	x	x	x
Death Valley	x	x	x	x
Dune Sands-North Algeria	-	x	x	x
Lena Delta 1998 no C org	x	x	x	x
Lena Delta 2002 ct. C org	x	x	x	-
Lake El'gygytgyn stream fill	*	*	x	x
Lake El'gygytgyn wet beach terrace	*	*	x	x
Lake El'gygytgyn dry beach terrace	*	*	x	x

*** = whole rock – bedrock samples from Lake El'gygytgyn**

x = performed

- = not performed

3.1 EXPERIMENTAL SETTING AND EQUIPMENT

A range of equipment and methods have been used to perform this cryogenic experiment. The seven samples from Ayers Rock - Australia, dune sands from North Algeria, Death Valley - USA, and Russian Federation (2x Lena Delta, 2x Lake El'gygytgyn) were separated in two

main grain sizes fractions of 32-63 µm and 63-125 µm, using various screens sieves with different stitches to separate the coarse and fine grains by adding regular tab water grain size separation (Figure 5). The grain size separation is useful for comparing single grains of the same grain size fraction in various samples instead of analyzing the bulk sample. After separation, the fractionated samples were placed in several evaporation dishes and put into a compartment dryer.

In the framework of this experiment, the organic compounds of the Lena Delta 1998 sample, which was already low (TOC=<0.1 %), had been mostly removed (same procedure as for SEM preparation) compared to Lena Delta 2002. The high amount of organics of 3.4 % TOC in the Lena Delta 2002 was left in the sample to compare the degree of quartz disintegration with the organic free sample. The organic compounds of the other samples were below TOC detection limit of 0.1 wt% that a chemical removal was not necessary.

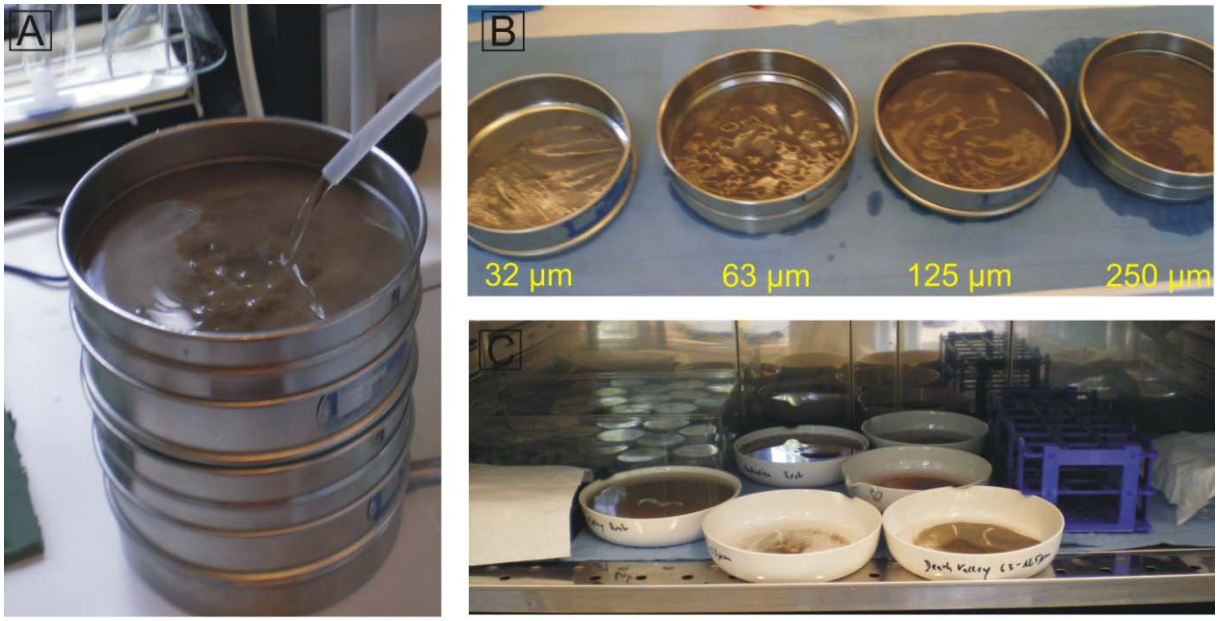

Figure 5: (A) Grain size separations using various riddle screens. (B) The separated grain sizes were dried in (C) a compartment dryer.

For the cryogenic experiment, the samples from Ayers Rock, dune sands- North Algeria, Death Valley as well as the Lena Delta (2x) and Lake El'gygytgyn (3x) in the grain size fraction 63-125 µm were placed in separate evaporation dishes. One sample from Lake El'gygytgyn beach terrace was left dry to assess the impact of thermal stress only on quartz grains. The other seven samples have been treated with distilled water. The water content was adequate enough to wet all material with a thin water film on top of the samples. Further,

the eight samples in the evaporation dishes were covered by aluminum foil to prevent contamination effects. The samples were put into the freezer with a constant temperature of -20°C. After 5-6 hours the frozen samples were taken out of the freezer and put into the compartment dryer. The temperatures in the compartment dryer varied between 25°C and 30°C. After about 18 hours the now dry samples were removed from the compartment dryer, refilled with distilled water and put back into the freezer. These F/T cycles were repeated 231 times with the thermal shock of temperature changes up to 50°C.

3.2 METHODS

Several methods have been used to investigate the effects of cryogenic weathering on the used samples from Ayers Rock, Death Valley, Dune Sands-Algeria, Lena Delta and Lake El'gygytgyn. An overview of the single separation steps is illustrated in Figure 6. The following sections describe the preparation, aim and technical details of these methods.

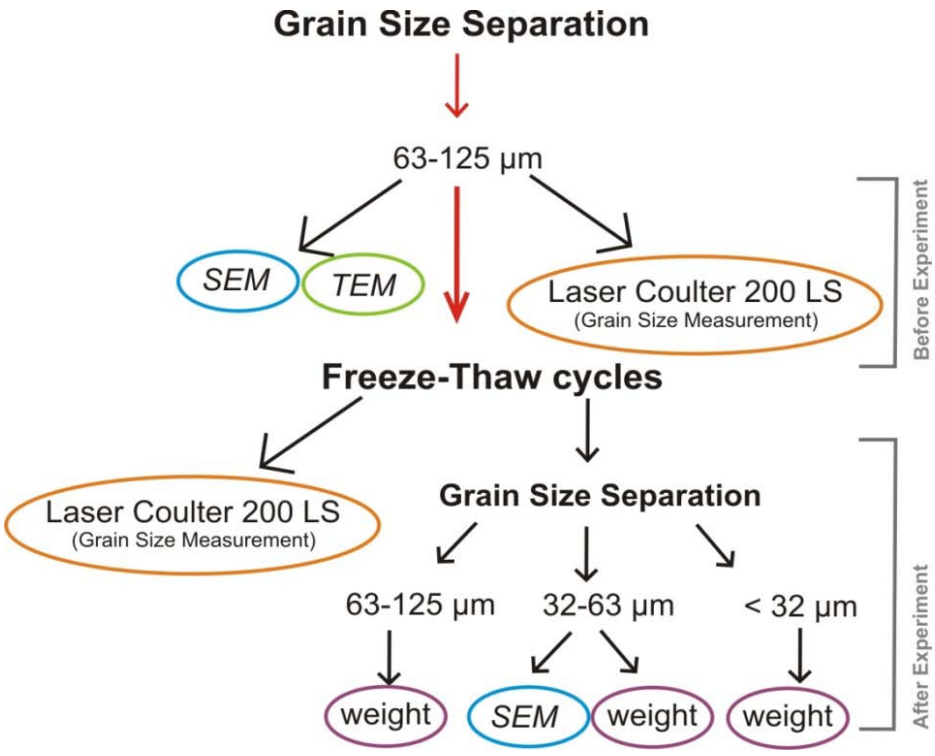

Figure 6: Laboratory protocol of the cryogenic experiment

3.2.1 TRANSMISSION ELECTRON MICROSCOPE (TEM) & OPTICAL MICROSCOPY (OM)

The TEM is a useful tool to investigate the microstructures of minerals in this cryogenic experiment, especially regarding possible lattice defects and inclusions within quartz grains. The aim of these two methods (TEM & OM) is to determine microstructural weakness zones of quartz, which may help explaining mineral fragmentation under cryogenic conditions. Similar studies of quartz grain microstructures have been only performed by Fliervoet, et al. (1997) compared to several fluid inclusion studies (e.g. Wilkins, et al. 1978, Walderhaug, 1994).

TEM & OM PREPARATION

The usage of the TEM and OM requires several steps of preparation. From the cryogenic experiment, five samples which have been obtained before the initiation of the freeze-thaw cycles (Lena Delta, dune sands- North Algeria, Ayers Rock, Death Valley) were kindly prepared by Anna Giribaldi to thin sections in the geological laboratory facility at the Freie Universität in Lankwitz, Berlin. From the Lake El'gygytgyn two thin sections from whole rocks were already available (see Figure 4), kindly provided by Dr. Georg Schwamborn from the Alfred Wegener Institute Potsdam. These rocks consist of quartz minerals which have not been experiencing cryogenic weathering on a micro scale and are important to investigate minerals before entering grain disintegration effects caused by transportation and weathering. The *OM* method has been used as an additional feature and supporting information to investigate the microstructures of quartz grains.

For the TEM method, the five thin sections and the two from the Lake El'gygytgyn have been further processed with great support of Dr. Richard Wirth at the Geoforschungszentrum (GFZ) Potsdam (Figure 7). The seven thin sections were coated with carbon to prevent isostatic charge. After this process, areas marked for further investigation have been cut out off the samples using Focused Ion Beam (FIB) technology and the *"Lift-out"* technique for sample preparation (Lie, et al., 2006). At the GFZ they use a FEI FIB200TEM for sample preparations. The *"Lift-out"* technique is useful for fragile or sensitive to contamination samples because the bulk sample is virtually touched compared to the conventional *"H-bar"* technique (Lie, et al., 2006). From these thin sections one to two thin quartz grain foils were

extracted to investigate lattice defects on a micro scale. Unfortunately quartz is very sensitive to radiation causing the quartz grains to be partly destroyed during the investigation.

TECHNICAL FEATURES OF THE TEM

The TEM is an advanced microscopy (Figure 7) technique capable of imaging at significant higher resolutions than light microscopy. The TEM method is based on transmitting a beam of electrons through sample material and measuring the resulting interaction of the sample with the beam. The interaction with the material forms an image of the sample by the electrons transmitting through the sample (Lie, et al., 2006).

Figure 7: (A) Sample preparation using a FEI FIB200TEM. (B) A FEI Tecnai™ G2 F20 X-Twin with a HAADF Detector has been used for visualizing microstructures on quartz. (Both pictures are the courtesy of the GFZ Potsdam.)

The processed foils in the order of 50 x 50 x 50 µm in size have been transferred to the TEM grid. The used TEM machine is a FEI Tecnai™ G2 F20 X-Twin with a HAADF Detector.

3.2.2 GRAIN SIZE MEASUREMENT-LASER COULTER LS 200

The Laser Coulter LS 200 is a semi-quantitative method and is used to measure grain sizes from loose particles. This method has been applied in numerous studies to evaluate grain sizes (e.g. Beuselinck, et al., 1998, Loizeau, et al., 1994, Stefano, et al., 2010) for soil genetic studies and comparative grain size distributions. The aim of these grain size measurements is to quantify grain size changes before and after the F/T cycles.

GRAIN SIZE MEASUREMENT - PREPARATION

The grain size measurements have been conducted with great support from Ute Bastian from the Alfred-Wegner Institute in Potsdam. The grain size measurement was performed twice- before and after the F/T cycles. The separated grain size fraction 63-125 µm before the initiation of freeze-thaw cycles were measured and were compared with grain size measurements of the samples after the cryogenic experiment. Before and after the F/T cycles a small part (filled spoon) of all used samples has been homogenized and mixed with regular tab water to bring the sample into suspension. The suspension with the sample was put into the opening of the Laser Coulter and measured 2-3 times to validate the results.

TECHNICAL FEATURES OF THE LASER COULTER LS 200

The Laser Coulter LS 200 is a diffraction particle size analyzer which can measure particles from 0.375 to 2000 µm. The technique is based on the Frauenhofer diffraction and Mie's theory of light scattering. For more information please read „Particle Size Measurement: Powder sampling and particle size measurement" from Allen (1998).

3.2.3 SCANNING ELECTRON MICROSCOPE (SEM)

The SEM is a useful method to investigate the grain surface and shapes of minerals. For the cryogenic experiment, the SEM has been use to investigate the effects of cryogenic

weathering upon quartz grains. This method is scientifically established and was used by Krinsley & Doorkamp (1973), Mahaney, et al. (1996), Van Hoesen, et al. (2004) to investigate grain shapes and variations under cryogenic conditions mostly in glacial areas. Culver, et al. (1983) in addition, analyzed quartz grain surface textures by using statistical approaches which have also been used as an additional tool for quartz surface changes.

SEM PREPARATION

For the SEM method, about 5 g (grain size fraction 63-125 µm) of each sample from Ayers Rock, dune sands, Death Valley, Lena Delta and Lake El'gygytgyn beach terrace and stream samples was obtained before and after (grain size fraction 32-63 µm) the initiation of the cryogenic experiment. The aim of this method is to investigate the changes in the micromorphology of quartz grains *after* experiencing cryogenic weathering. In addition, after the F/T cycles, the dry sample from Lake El'gygytgyn beach terrace has also been used to investigate the thermal stress effects on quartz.

The usage of the SEM requires previous cleaning of the samples. All the samples have been decanted and washed about 10 min in SnCl2 (5%) to remove iron and organics; and after the samples were cleaned with distilled water and put in an ultrasonic bath (2 min), and then added 5% HCL for 5 min to remove carbonate before washing again (modified after Schirrmeister, 1995). After drying the samples, about 20 quartz grains have been separated using a preparation needle. Further, the separated quartz grains were placed on an aluminum tub, which is about 1.0 cm in diameter. To visualize sample material with the SEM, their surfaces must be electrical conductive and electrical grounded to prevent the accumulation of electrostatic charge at the surface. Therefore the seven samples have been coated with gold by a low vacuum sputter. Gold has a high atomic number and a high electrical conductivity and is therefore ideal for the SEM.

TECHNICAL FEATURES OF THE SEM

With great support from Jan Evers of the Paleontology department at the Freie Universität Berlin, the visualizing of the samples has been performed by a Zeiss Supra 40VP with Gemini

technology (Figure 8). The Zeiss Supra 40VP is a scanning electron microscope with an Everhart Thornley secondary electron detector device (Figure 8). The scanning electron microscope (SEM) uses a focused beam of high-energy electrons which generate at the surface of solid specimens signals that derive from electron-sample interactions (Watts, 1985). This reveals information about the sample including external micromorphology, chemical composition, and crystalline structure and orientation of materials making up the sample.

Figure 8: SEM aperture located at the Paleontology Department of the Freie Universität, Berlin (courtesy: J. Evers).

The SEM generates deep focus images of a about less than 1 to 5 nm in size of sample surfaces. The Everhart Thornley secondary electron detector is a scintillator that emits photons when sample material gets hit by high-energy electrons. The emitted photons are collected by a light-guide and transported to a photomultiplier for detection (Watts, 1985).

4 RESULTS

For the length of the cryogenic experiment, eight samples have been frozen and thawed 231 times. The F/T cycles took place on a regular time schedule to replicate seasonal temperature changes in the upper layer (active layer) of the permafrost soil. Grain size measurements, micromorphological (SEM) and structural (TEM & OM) analyses have been performed to investigate the effects of cryogenic disintegration on quartz breakup.

4.1 GRAIN SIZE ANALYSIS

Before and after the F/T cycles, grain size measurements were undertaken for all samples using the Laser Coulter. Due to the limitation of this method by showing variations in their results, the measurements have been performed at least 2-3 times to calculate an average measurement. All displayed results have been converted from volume percent (vol %) into percent (%) by calculating the changes from before to after the F/T cycles. An overview of all LS results is displayed in figure 9 as well as in the appendix.

For the *Ayers Rock* samples, grain size measurements show an increase in the fraction <32 µm of +6.6 % after the F/T cycles (Figure 9) in comparison to before the F/T cycles. In particular in the fraction 32-63 µm show enrichment in the silt fraction of up to +7 %. The laser particle sizing results in the *Death Valley* shows only a slight growth (+0.6 %) in the fraction < 32 µm after the F/T cycles. Moreover, in the Death Valley sample there is a volume decrease in the fraction 32-63 µm of -0.8 %. The fraction 63-125 µm indicate only a small increase of +1.32 % for Death Valley but there is no increase being observed in the grain size fraction smaller than 63 µm. Moreover, the *dune sands of North Algeria* reveal after the F/T cycles an volume increase in grain size fraction > 125 µm of +4.2 %. Changes in the smaller grain size fractions < 125 µm conclude only decreases in these fractions. Similar observations have been noted in the grain size measurements of *Lake El'gygytgyn dry beach terrace*

because like for the dune sands of North Algeria, is an increase for >125 µm and a decrease in all smaller fractions reported.

Grain size analyzes of the *Lena Delta* samples show significant changes in the grain size distribution between Lena Delta 1998 and 2002. As shown in figure 9, the percent changes in the Lena *Delta 2002 ct C org* samples illustrate an increase in the fractions <32 µm of 4.4 %. The *Lena Delta 1998* samples reveal an increase of +1.17 % in the <32µm fraction. For Lena Delta 1998 there is a volume decrease of -0.62 % in the fraction 32-63 µm implying a loss of grain sizes in this fraction. The Lena Delta 2002 instead shows an increase of +9 % in the fractions 32-63 µm. As expected from the enrichment of the fractions <63 µm after the F/T cycles, a decrease in the Lena Delta 2002 sample of -12 % is recorded in the fractions 63-125 µm. For the *Lake El'gygytgyn beach terrace (wet sample)*, strong increases in the grain size fractions < 32 µm of +18.3 % are observable after the F/T cycles. The beach terrace wet sample show the highest changes in grain size than any other sample from this experiment. Furthermore, in the fractions 32-63 µm of +7.2 % there is a volume increase in the beach terrace wet sample reported.

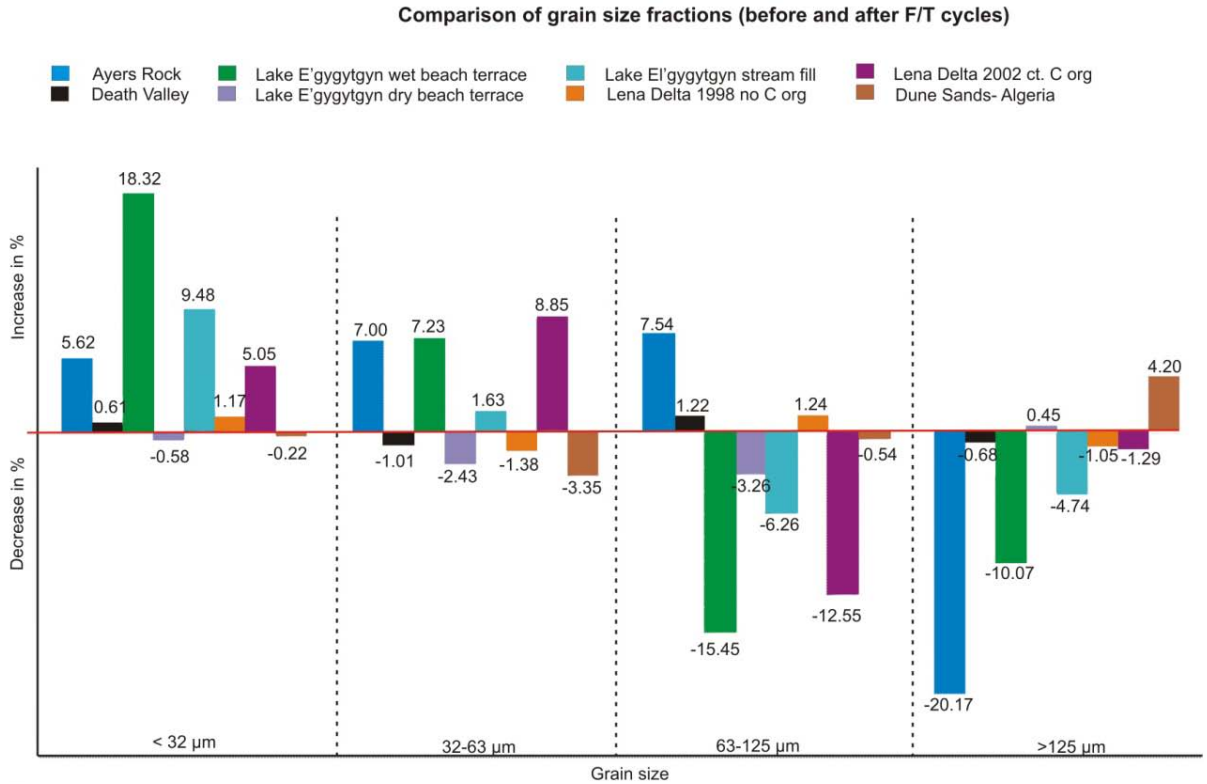

Figure 9: Summary of percental changes in grain size distribution of all samples performed by the Laser Coulter LS 200 after the freeze-thaw cycles and compared with before the F/T cycles.

The grain size analyses from *Lake El'gygytgyn stream samples* indicate an increase in the <32 µm fraction of +9.6 %. Further, the increase in the fraction 32-63 µm is significant low by only +1.63 % compared to the beach terrace wet sample. Summarizing, decreases in grain size fractions 63-125 µm of -6.26 % and in grain size fractions > 125 µm of -4.74 % correspond to the enrichment in the silt fraction < 63 µm in the Lake El'gygytgyn stream fill samples

GRAIN SIZE MEASUREMENT – USING ANALYSIS SCALE

Due to the limitation of the Laser Coulter, another approach to estimate grain size change has been used to differentiate the obtained LS results.

After the F/T cycles, all samples were separated into three grain size fractions (< 32 µm, 63-32 µm, 125-63 µm) using various screen sieves (see Chapter 1, Figure 6). Afterwards, the three different grain size fractions were weighed to scientific precision using a laboratory scale. The obtained results are displayed in gram (g) and then converted into weight percent (wt %) by using the total weight of each sample as 100 wt % (Figure 10). The displayed wt % also show increases in the grain size fraction < 63 after the F/T cycles because before the F/T cycles only one grain size fraction (63-125 µm) was used for this cryogenic experiment.

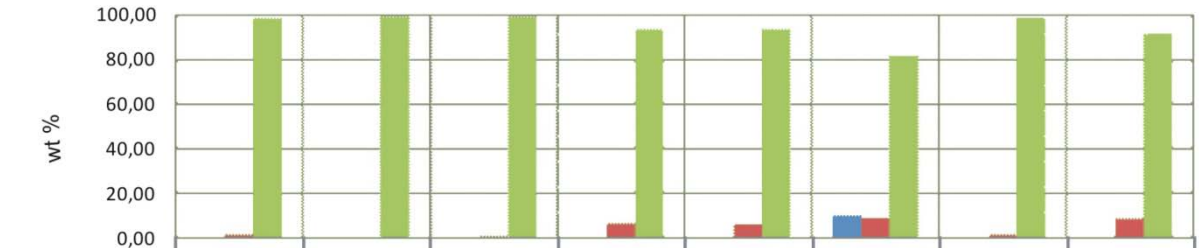

	Algeria	Australia-Ayers Rock	USA-Death Valley	Lake El'gygytgyn beach terrace	Lake El'gygytgyn beach terrace (DRY)	Lake El'gygytgyn stream fill	Lena Delta 1998 no C org	Lena Delta 2002 C org
wt %<32 µm	0,11	0,31	0,20	no data	no data	9,71	no data	no data
wt % 32-63 µm	1,24	0,40	0,60	6,29	6,21	8,66	1,16	8,43
wt % 63-125 µm	98,66	99,29	99,20	93,71	93,79	81,63	98,84	91,57

Figure 10: Summary of all samples weighed after the experiment. Please note, for Lake El'gygytgyn beach terrace and Lena Delta 1998/2002 grain size fraction <32 µm has been measured with the fraction 32-63 µm.

For the *dune sands of North Algeria*, the weight results indicate an increase of the smaller grain size fractions <63 µm (1.34 wt %) compared to the results from the Laser Coulter LS 200. Further, grain size fraction < 32 µm in the *Ayers Rock* sample illustrate only small increases of 0.31 wt %. Similar increases in the enrichment of the fraction 32-63 µm have been seen in *Ayers Rock* samples of 0.71 wt % in the fraction < 63 µm and are consequently dominated in grain size fraction 63-125 µm (Figure 10). The *Death Valley* samples reveal in comparison with the *Ayers Rock* almost identical results in grain size distribution after the F/T cycles (see Figure 10) of 0.80 wt % in the grain size fraction < 63 µm.

The *Lake El'gygytgyn dry beach terrace* samples displays a strong increase in the grain size fraction <63 µm of 6.21 wt %. The *Lake El'gygytgyn wet beach terrace* samples has almost identical grain size distribution in < 63 µm of 6.29 wt %, also observable in figure 10. Further, the *Lake El'gygytgyn stream fill* samples show strong enrichment of >18 wt % in the smaller grain size fractions < 63 µm and correspond to the observations of the Laser Coulter. On the contrary, the *Lena Delta* samples reveal strong variations in comparison with *Lena Delta 1998* and *2002*. The *Lena Delta 1998* shows only a small enrichment in the grain size fraction < 63 µm of 1.2 wt % compared to the *Lena Delta 2002* of 8.4 wt % which corresponds to the results of the Laser Coulter.

4.2 MICROMORPHOLOGY OF QUARTZ GRAINS BASED ON SEM ANALYSES

The microstructural analyses have been performed using the interpretation key of Krinsley and Doornkamp, (1973). Feature counting has been completed before and after F/T cycling. However, an interpreter´s bias cannot be fully excluded when highlighting presumably newly formed grain micromorphological features due to the F/T grain breakup.

DUNE SANDS- NORTH ALGERIA

Quartz grain shapes from the North Algeria Dune Sands (Figure 11 A) *before the F/T cycles* are dominated by subrounded to minor subangular shapes. Commonly elongated shapes occur. Marked by minor large conchoidal fractures as well as in breakage blocks, they show

regularly observable surface features of precipitation effects, marked by subrounded pits (Figure 11 A-inset). They may result from grain-to-grain drumming or chemical dissolution. Arc-shaped steps are seen in the half of all samples from North Algeria.

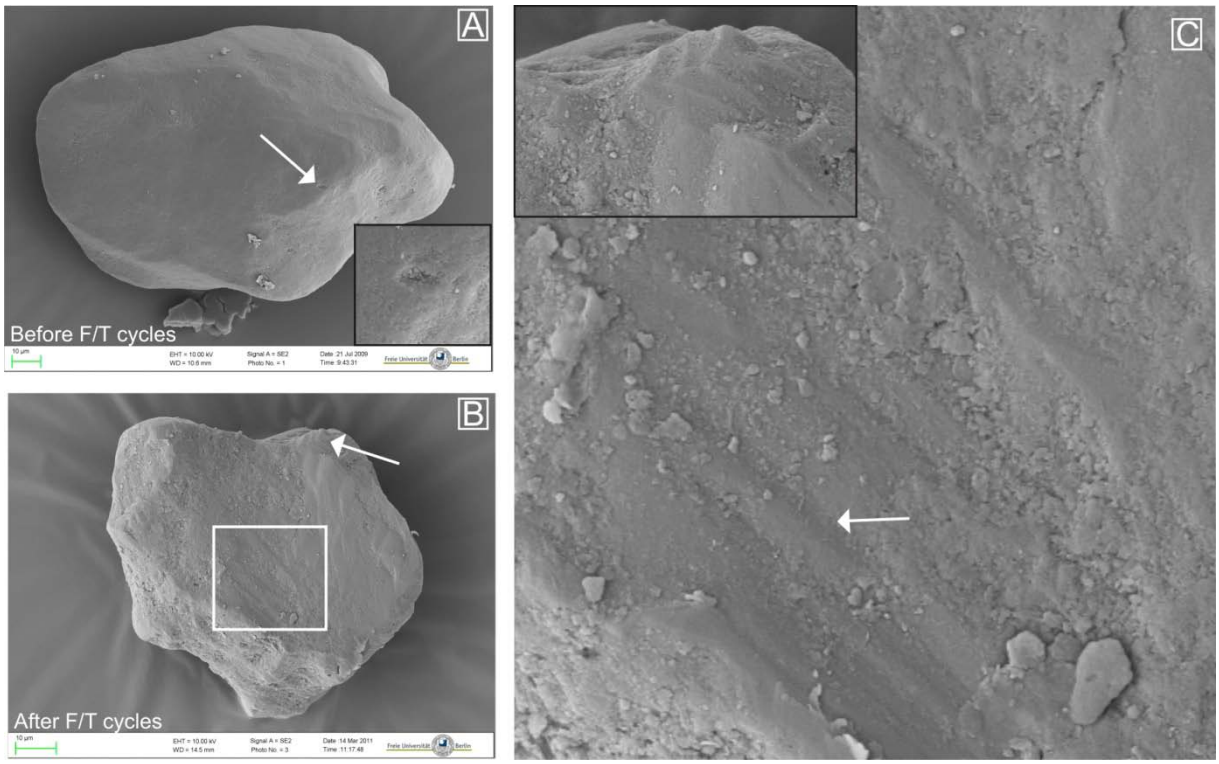

Figure 11: Micromorphology of the North Algerian dune sand quartz grains. *Before F/T cycles*: (A) Quartz grain shape is subrounded and shows small scaled cracks (arrow and black inset). *After F/T cycles:* (B) Quartz grain is characterized by a relative sharp sub-angular shape and breakage block features along the grain corners. Note the well defined arc-shaped steps (arrow and white inset) and the linear fractures displayed and enlarged in (C) the white inset. The black inset is an enlargement of (B-white arrow), showing parallel, linear arranged steps.

Occasionally, the observed quartz grains *after the F/T cycles* small conchoidal fractures as well as breakage blocks can be seen (Figure 11 B). Close to these small conchoidal fractures, parallel and linear fractures are frequently observable (Figure 11 B-C). Precipitation features as occasionally observed before the F/T cycles are rarely visible after the F/T cycles.

AYERS ROCK - AUSTRALIA

The Ayers Rock samples *before the F/T cycles* show strong variations in quartz grain shapes from rounded to sub-angular. In addition, some of the quartz grains have elongated shapes. Surface features of curved and straight grooves are rarely seen compared to arc-shaped

steps which occur frequently (Figure 12 A). Conchoidal surface features are rarely visible corresponding to the minor presence of breakage blocks.

After the F/T cycles, the observed quartz grains from Ayers Rock is marked by complex shape and surface features. The quartz shapes are angular thus few rounded grains also occur. The quartz grains from Ayers Rock show a strong occurrence in breakage block features as well as in conchoidal fractures (Figure 12 B-C). These conchoidal fractures show in some of the quartz grains intense fracturing associated with cleavage planes (Figure 12 B-C).

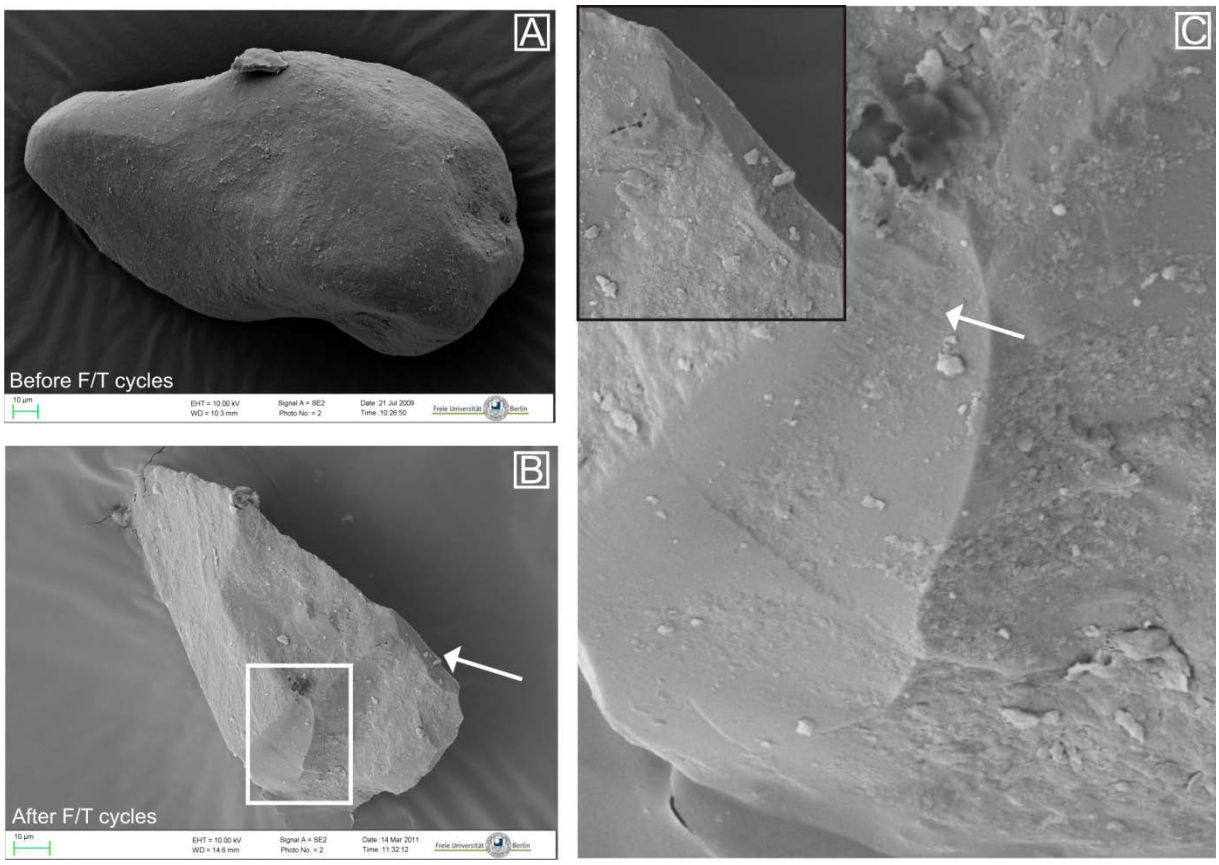

Figure 12: Micromorphology of Ayers Rock (Australia) quartz grains. *Before F/T cycles*: (A) Aeolian quartz grain with sub-rounded and elongated shape. Minor fractures are shown. *After F/T cycles:* (B) Angular quartz grain with small cleavage plane (arrow) as well as conchoidal features displayed in (C) the white inset, subparallel linear fractures (arrow). The black inset in the upper left corner is an enlargement of B (white arrow) showing a typical sharp defined cleavage plane.

DEATH VALLEY - USA

Before the F/T cycles, quartz grains from Death Valley have abundant angular to sub-angular grain shapes and are minor sub-rounded (Figure 13 A). The observed quartz grains show

with great regularity breakage block features as well as conchoidal fractures (Figure 13 A). These conchoidal fractures are commonly associated with subparallel linear fractures as well as in curved and straight grooves. Oriented scratches and grooves with linear steps appear with great regularity. In addition, minor precipitation features with solution pits have been seen and are shown in figure 13.

After the F/T cycles, the surface features of the observed quartz grains from Death Valley minor angular shapes but common sub-rounded edges (Figure 13) marked by small breakage blocks. Further, numerous amounts of large conchoidal fractures but also of cleavage planes are dominant features of the analyzed quartz grains. Typical large breakage blocks and arc-shaped steps were as frequently observed as in before the F/T cycles. As shown in figure 13 (C), micro cracks are seen in the Death Valley sample. But it is not clear if this is due to the F/T cycles of this experiment, or if it is a result of previous weathering effects in the deposit area.

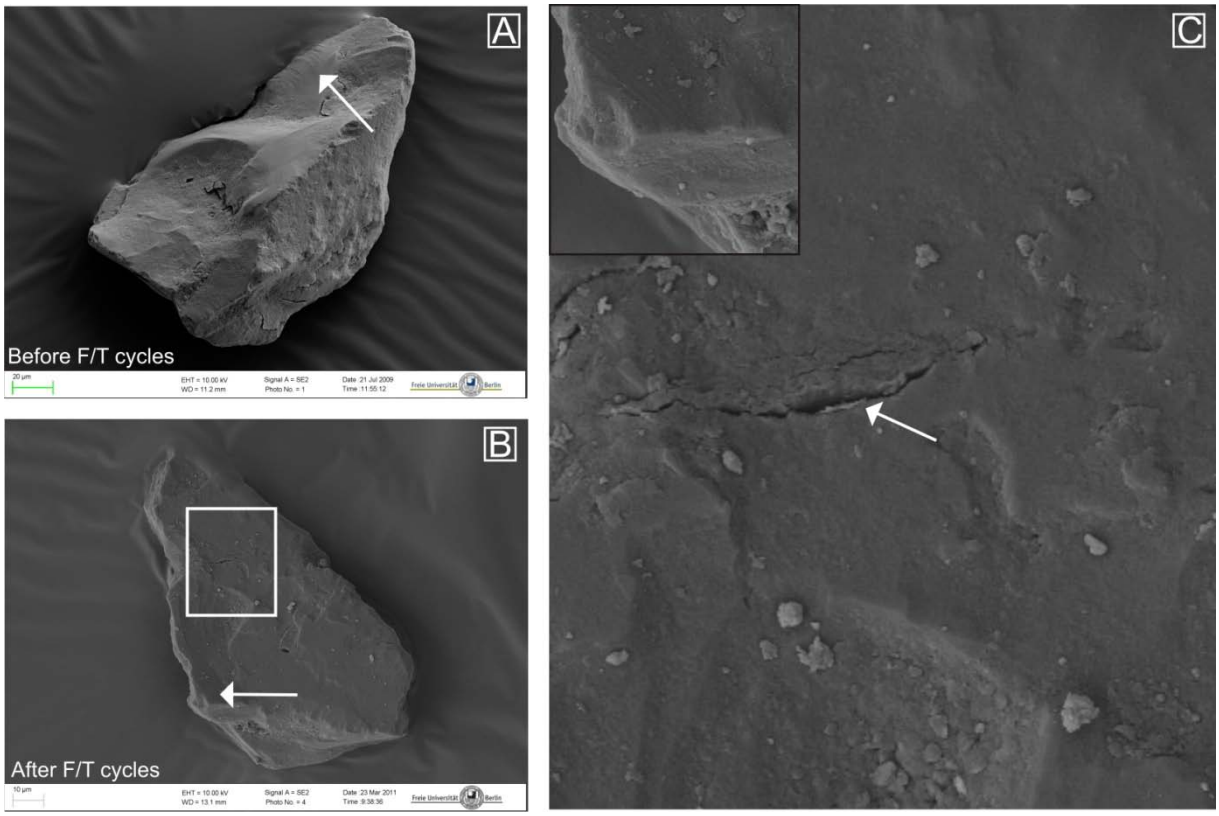

Figure 13: Micromorphology of Death Valley (USA) quartz grains. *Before F/T cycles:* (A) Quartz surface with large conchoidal fractures (see arrow). *After F/T cycles:* (B) Arc-shaped steps (arrow) with parallel linear and conchoidal fractures. (C) The white inset is an enlargement from B (white frame): possible cryogenic cracks in quartz accommodated along arc-shaped steps (arrow). The black inset is an enlargement of B (arrow) displaying in the upper left corner small breakage blocks which are accommodated by arc-shaped steps.

LENA DELTA – RUSSIAN FEDERATION

The quartz grain surface features from the Lena Delta *before the F/T cycles* show dominantly subrounded and in particular in subangular shapes. Quartz grain surface features from Lena Delta are dominated by conchoidal fractures accommodated by abundant breakage blocks and arc-shaped steps (Figure 14 A-B). Further, curved groove features in Lena Delta quartz grains are frequently seen and observable in Figure 14 B.

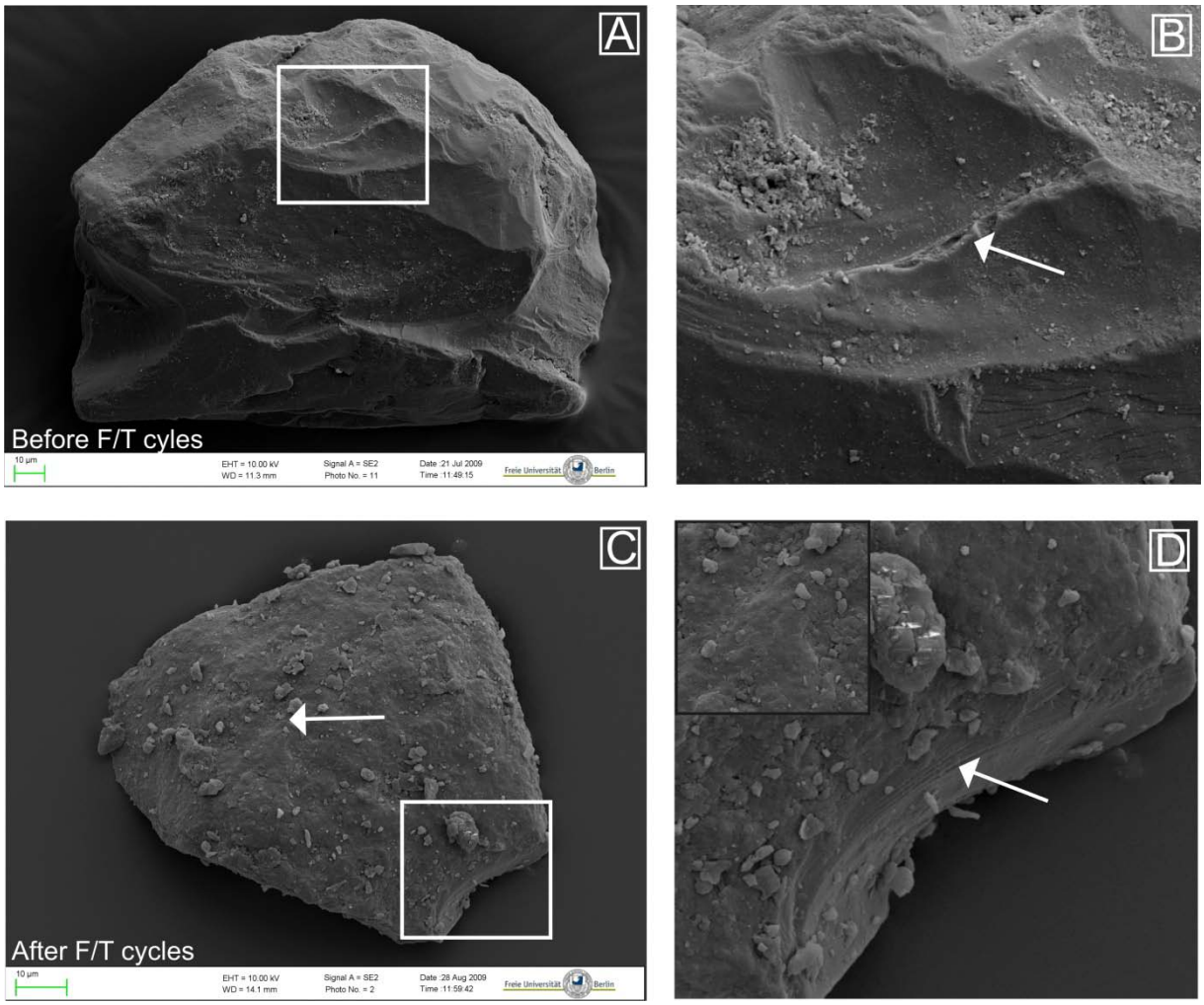

Figure 14: Micromorphology of Lena Delta quartz grains. *Before F/T cycles*: (A) Subrounded quartz grain with conchoidal fractures and curved grooves. The white inset is enlarged in (B) showing quartz breakup features of arc-shaped steps (arrow). *After F/T cycles*: (C) Precipitation features combined with fresh breakage blocks. The white inset is enlarged in (D) showing large breakage blocks along subparallel linear fractures (arrow). The black inset in the upper left corner is an enlargement of (C)-white arrow displaying precipitation features presumably silica based.

After the F/T cycles, the observed quartz grains from Lena Delta shows dominantly sub-angular to sub-rounded shape features. In addition, large breakage block fractures as well as corresponding conchoidal and precipitation features are observable (Figure 14 C-D).

LAKE EL'GYGYTGYN STREAM FILL – RUSSIAN FEDERATION

Quartz grain analyzes from Lake El'gygytgyn stream fill *before the F/T* cycles show abundant angular shapes as well as subangular shapes to a minor amount. Surface analyzes illustrate extensive fracturing and abrasion features shown with conchoidal fractures and accompanied by frequently seen large breakage blocks.

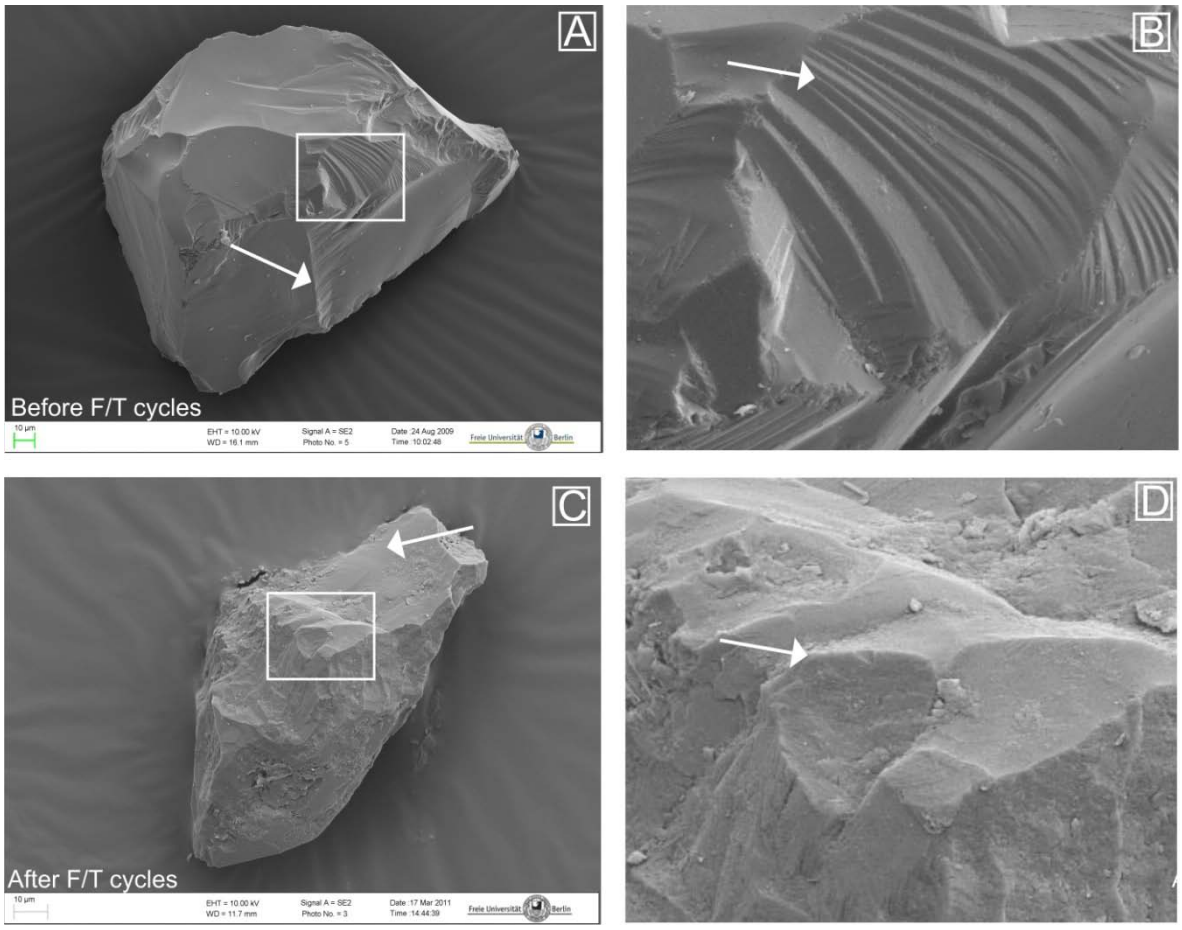

Figure 15: Micromorphology of Lake El'gygytgyn stream fill quartz grains. *Before F/T cycles*: (A) Fracture face in El'gygytgyn quartz with conchoidal fractures (central). The arrow is pointing to a sharp linear fracture. An enlargement of the white inset is shown in (B). This area is marked by sub-parallel arc-step fractures and abrasion features. *After F/T cycles:* (C) Subangular quartz grain with extensive abrasion and breakage block features. In addition, large conchoidal fractures (arrow) occur frequently. The white inset enlarged in (D) shows well defined curved grooves along random scratches and grooves (arrow).

Moreover, linear- and arc-shaped steps have been seen regularly along conchoidal fractures. These features are also displayed in figure 15 A-B.

After the F/T cycles, quartz grain shapes from Lake El'gygytgyn stream fill show no significant changes-dominated by angular to subangular grain shapes (Figure 15 C-D). Further, conchoidal fractures are observed more frequently than arc-shaped steps which appear on a regular basis. On the contrary, straight grooves occur regularly along with curved grooves (Figure 15 C-D). Typical breakage blocks which are in relationship with the occurrence of conchoidal fractures appear as regular as before the F/T cycles. In addition, precipitation features marked by solution pits and hollows are a rare feature within this sample.

LAKE EL'GYGYTGYN BEACH TERRACE – RUSSIAN FEDERATION

The quartz grains from Lake El'gygytgyn beach terrace *before the F/T* cycles show in comparison with the stream fill samples similar micromorphological features. The quartz grains of the Lake El'gygytgyn beach terrace before the F/T cycles are defined by commonly observed angular shapes. The quartz grains from the Lake El'gygytgyn beach terrace show a regular occurrence of conchoidal fractures. These conchoidal fractures are also shown in figure 16 A-B. In addition, subparallel linear fractures occur frequently close to the conchoidal fractures (see Figure 16 B) and are mostly bound by the commonly seen breakage blocks.

After the F/T cycles, most of these Lake El'gygytgyn beach terrace quartz grain samples (wet & dry) show similar shapes of quartz grains features as observed before the F/T cycles; mostly they are marked by angular to sub-angular shapes (Figure 16). Surface features show common occurrence of conchoidal fractures and breakage blocks. Parallel linear fractures in quartz appear frequently in the wet and dry samples from Lake El'gygytgyn beach terrace. At the corners/edges of quartz grains, abrasion features have been regularly seen. These abrasion features are marked by small scale breakup features concentrated along the edges of the quartz grains. Compared to the wet sample, the dry sample shows more precipitation features on quartz grains which are marked by solution pits.

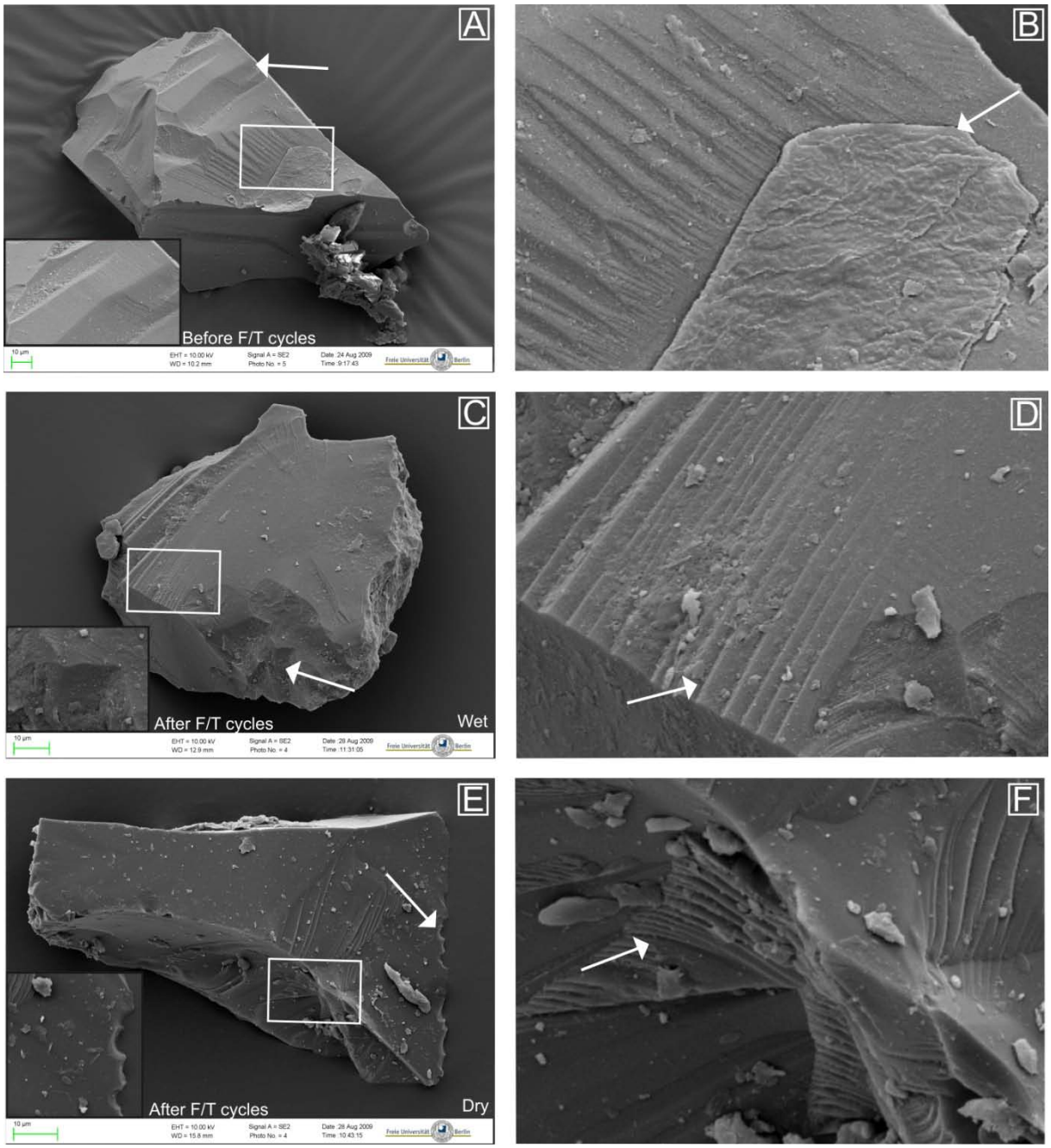

Figure 16: Micromorphology of Lake El'gygytgyn beach terrace quartz grains – *Before F/T cycles:* (A) Fracture face on an angular quartz grain with subparallel linear fractures (center and arrow) and whole plate detachment (top left and right). The black inset is an enlargement of the arrow showing linear and small conchoidal fractures. The white inset shown in (B) is displaying well defined subparallel, linear fractures (left part of the picture) interrupted by a detached plate (arrow). *After F/T cycles (wet):* (C) Angular to subangular quartz fragment with abraded grooves (top right) and fresh breakage blocks (arrow). These breakage blocks with sharp corners are shown in more detail in the black inset. Further, the white inset which is enlarged in (D) shows linear steps features (arrow) with curved grooves (lower right). *After F/T cycles (dry):* (E) Quartz grain is marked by large conchoidal features (center) with subparallel and linear fractures (center-right). The edges (arrow) point out prominent fresh but small breakage blocks. The white inset which is enlarged in (F), shows a well defined conchoidal fracture face with parallel linear to curved grooves.

4.2.1 STATISTICAL SURVEY

Statistical surveys of the quartz micromorphological features from all used samples before and after the F/T cycles have been performed to identify shape and surface changes due to possible cryogenic weathering effects. An overview of the used quartz grains is given in table 3. Due to time and preparation issues the amounts of analyzed quartz grains is limited. Caused by that, the SEM method was not performed on the Lena Delta 2002 sample after the F/T cycles. Therefore, the here presented results its validity have to be treated with caution.

Table 3: Overview of the number of quartz grains used for the SEM and micromorphological evaluation

Sample/ Number of quartz grains	**Dune sands - Algeria**	**Ayers Rock - Australia**	**Death Valley - USA**	**Lena Delta 1998**	**Lena Delta 2002**	**Lake El'gygytgyn beach terrace**	**Lake El'gygytgyn WET beach terrace**	**Lake El'gygytgyn DRY beach terrace**	**Lake El'gygytgyn stream fill**
Before F/T cycles # of quartz grains	12	6	11	16	11	7	N.A.	N.A.	7
After F/T cycles # of quartz grains	6	5	6	3	-	N.A.	11	13	8

N.A.= not applicable

STATISTICAL SURVEY-CALCULATION

The total number of quartz grains per sample is taken as 100 %. The occurrence of shape and surface features were divided by the number of observed quartz grains per sample. Therefore, as an example from 10 quartz grains, 8 quartz grains have arc-shaped steps and 5 show precipitation features which correlate to 80 % arc-shaped steps and 50 % precipitation features.

RESULTS OF STATISTICAL SURVEY - QUARTZ GRAIN SHAPE FEATURES

Changes in quartz grain *shapes* after the F/T cycles have been in particular observed in the Ayers Rock and in the North Algeria dune sand samples (Figure 17). Before the F/T cycles,

the quartz grains of the North Algeria dune sands are dominated by sub-rounded shapes - 75 % of all quartz grains in this sample. After the F/T cycles the quartz grains of the North Algeria dune sands show a strong decrease in sub-rounded shapes to less than 10 % of the total and consequently and increase in sub-angular shapes to 80 % (Figure 17).

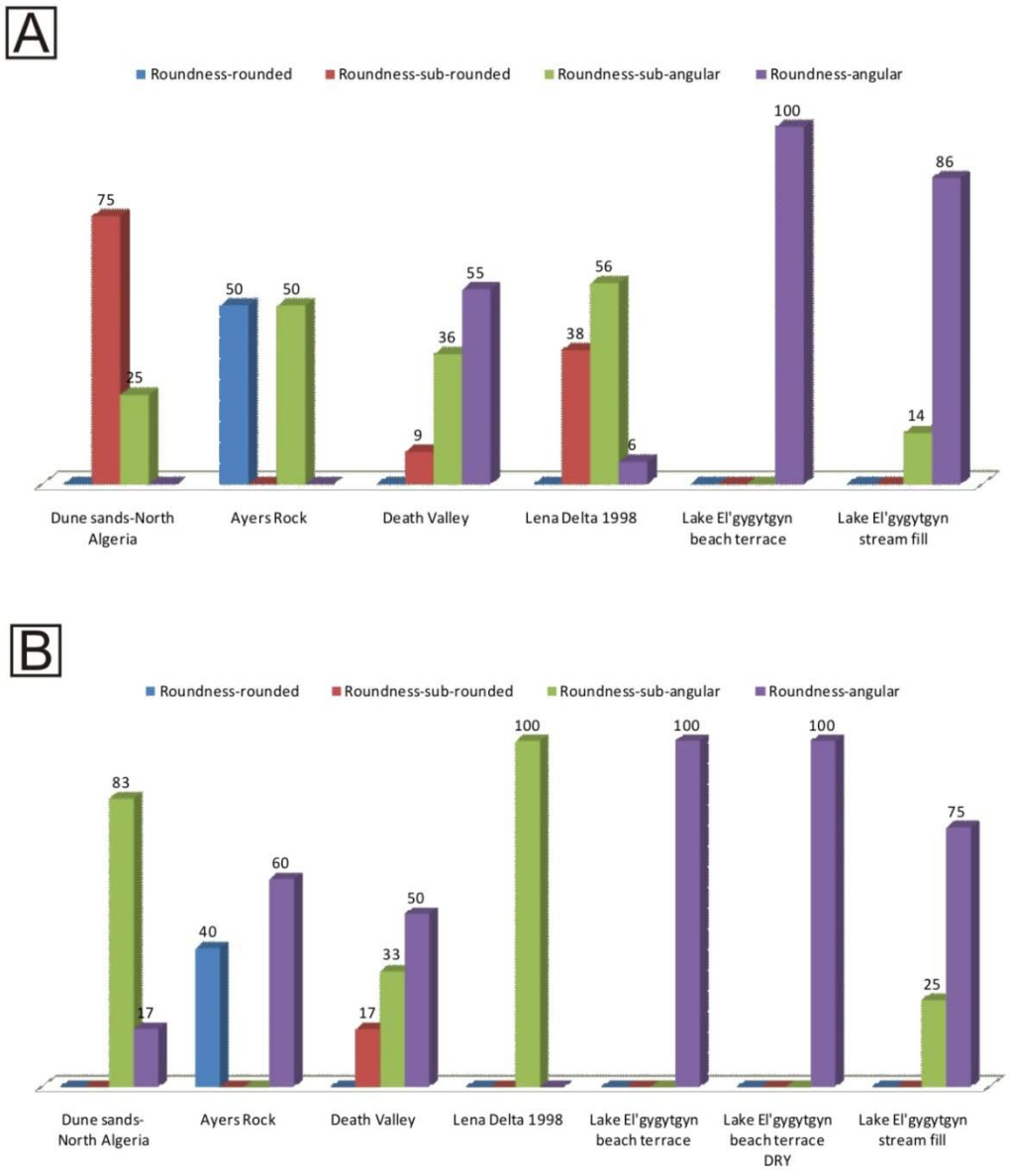

Figure 17: Statistical evaluation of quartz grain shape features from all samples (A) *Before* the F/T cycles (B) *After* the F/T cycles. All values are displayed as a percentage of the total number of grains of each sample.

Similar observations have been made in the Ayers Rock sample where a significant increase in angular shaped quartz grains was reported after the F/T cycles (see Figure 17). In addition, Death Valley and Lake El'gygytgyn show only minor changes in quartz grain shapes after the F/T cycles. Further, increases in breakup features after the F/T cycles have been statistically

noted in most of the observed quartz grains from Ayers Rock, Death Valley, dune sands-North Algeria and Russia (Lena Delta, Lake El'gygytgyn).

QUARTZ GRAIN SURFACE FEATURES

The non-periglacial samples from Ayers Rock, Death Valley and the dune sands from North Algeria, show in the analyzed quartz grains minor to medium increases in conchoidal fractures corresponding with the parallel linear fractures which increased ~20 % (Figure 18) to the observations before the F/T cycles.

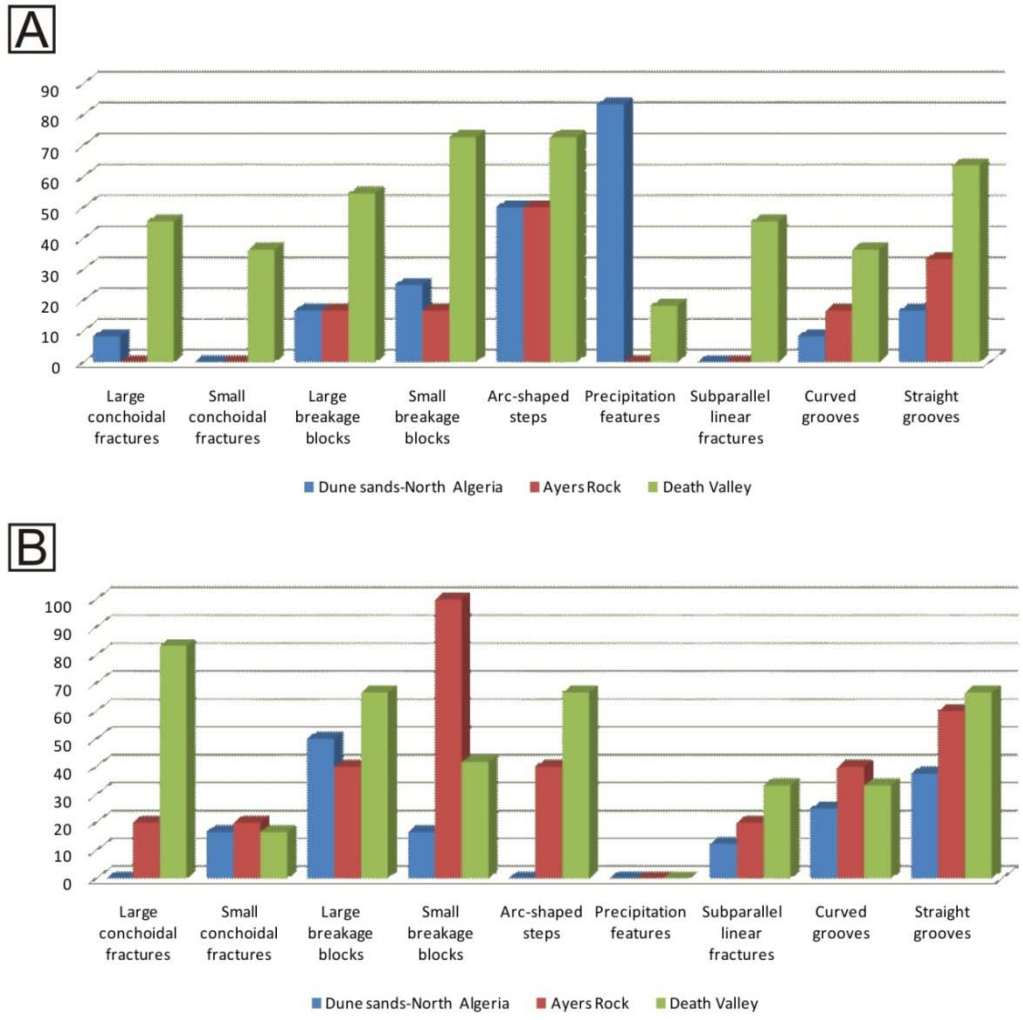

Figure 18: Quartz grain surface of the *non-periglacial* samples (A) *Before* and (B) *after* the F/T cycles. All values are displayed as a percentage of the total number of grains of each sample.

In addition, the amounts of breakage blocks increased significantly in the Ayers Rock quartz grains of up to 80 % though in Death Valley is reported a decrease of 20 % in breakage blocks

(Figure 18). The Death Valley quartz grains are commonly showing minor decreases (< 5 %) in the entire surface features except of the conchoidal fractures which increased to 18 %. Compared to the non-periglacial samples, the Lena Delta and Lake El'gygytgyn quartz grain micromorphology vary in their occurrence and intensity of breakup features (Figure 19). Surface features of the Lake El'gygytgyn vary from the stream fill as well as wet beach terrace and dry beach terrace quartz grain micromorphology. The Lake El'gygytgyn wet beach terrace quartz grains shows strong increases of up to 40 % in conchoidal fractures compared to the other Lake El'gygytgyn quartz grain samples.

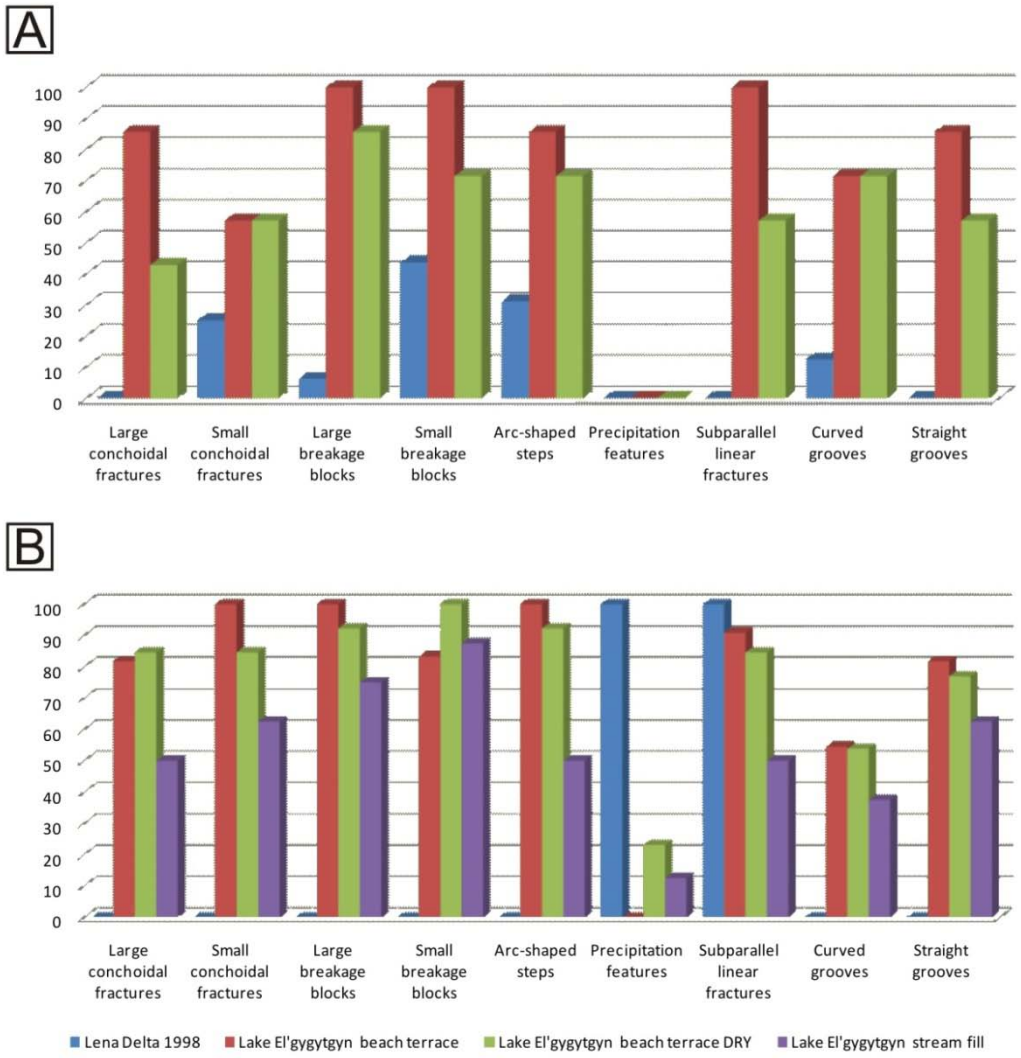

Figure 19: Quartz grain surface features of *periglacial* samples (A) *before* and (B) *after* the F/T cycles. All values are displayed as a percentage of the total number of grains of each sample.

In particular the Lake El'gygytgyn stream fill quartz grains are marked by an increase in conchoidal features of >60% and of around 70% in breakage blocks. The analyzed quartz

grains from the Lena Delta 1998 indicate large increases in precipitation features and subparallel linear fractures but also some decreases in other surface features.

SUMMARY OF STATISTICAL SURVEY

A summary of all obtained data is shown in table 4.

Table 4: Statistical data of micromorphological quartz features, displayed in percentage changes.

Category/ Sample	**North Algeria - Dune sands**	**Australia - Ayers Rock**	**USA - Death Valley**	**Lena Delta 1998**	**Lake El'gygytgyn (wet) beach terrace**	**Lake El'gygytgyn (dry) beach terrace**	**Lake El'gygytgyn stream fill**
Large conchoidal fractures	-8	13	38	0	-4	-1	63
Small conchoidal fractures	13	13	-20	25	43	27	63
Large breakage blocks	21	8	12	6	0	-8	75
Small breakage blocks	-13	46	-31	44	-17	0	75
Arc-shaped steps	-50	-25	-6	31	14	7	63
Precipitation features	-46	0	-18	0	0	23	63
Subparallel linear fractures	0	13	-12	0	-9	-15	-7
Curved grooves	-8	8	-3	13	-17	-18	-34
Straight grooves	8	4	3	0	-4	-9	5
Roundness-rounded	0	-25	0	0	0	0	0
Roundness-sub-rounded	-75	0	8	38	0	0	0
Roundness-sub-angular	38	-50	-3	56	0	8	11
Roundness-angular	13	38	-5	6	0	92	-11

The results of the statistical survey of Ayers Rock, dune sands from North Algeria, Death Valley and Russia (Lena Delta and Lake El'gygytgyn) show in all samples (partly) significant changes in shape and surface quartz micromorphology after the F/T cycles in comparison to before F/T cycles.

4.3 MICROSTRUCTURES OF QUARTZ GRAINS BASED ON TEM ANALYSES

The following microstructural analysis and results were performed following the methods of Hirth and Tullis (1992), Goltrant et al. (1991) and Bakker et al. (1994).

AYERS ROCK - AUSTRALIA

Microstructural analyses of quartz grains from Ayers Rock show distinct lattice defects, seen in subgrain boundaries and straight to curved dislocations. Theses straight dislocations are commonly observed within the quartz grain sample and seemed to accumulate along subgrain boundaries (Figure 20). The subgrain boundaries are identified by the diffraction contrast (black bands), which indicates in this case (Figure 20) a *low* angle subgrain boundary. Low angle boundaries are marked by weak to medium changes of the diffraction contrast along the two subgrains compared to *high* angle grain boundaries, which are characterized by a high diffraction contrast. High angle subgrain boundaries do not occur within this quartz grain.

Optical microscopy of the Ayers Rock sample shows that most of the quartz grains are subrounded to subangular whereas some of them having elongated shapes (Figure 21 A-B center). Microstructural features such as inclusion trains and bubbles are frequently seen in the thin section. In particular inclusion trails appear frequently as a pervasive feature in the quartz (Figure B-arrow). Unfortunately it was not possible to identify if the bubbles and trails include a fluid phase.

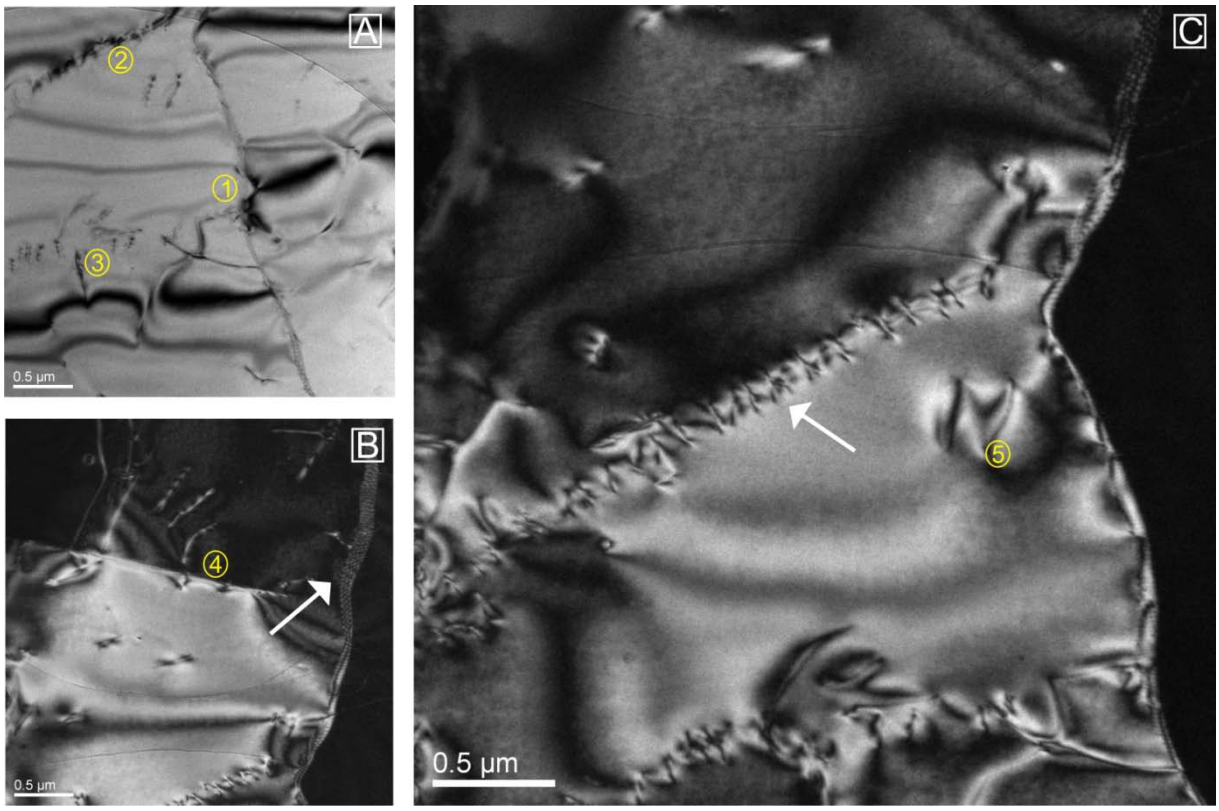

Figure 20: Microstructural analyses of Ayers Rock quartz grains. (A) Bright field micrograph. Two subgrain boundaries (1&2) occur with various dislocations (3). (B) Dark field micrograph. Lattice defects due to healing process led to subgrain formation (4) which is bounded by an inclusion trail (arrow) and accompanied with a medium to dense network of dislocations. (C) Several grain boundaries (arrow) and dislocations (5) appear frequently in this area of the quartz grain.

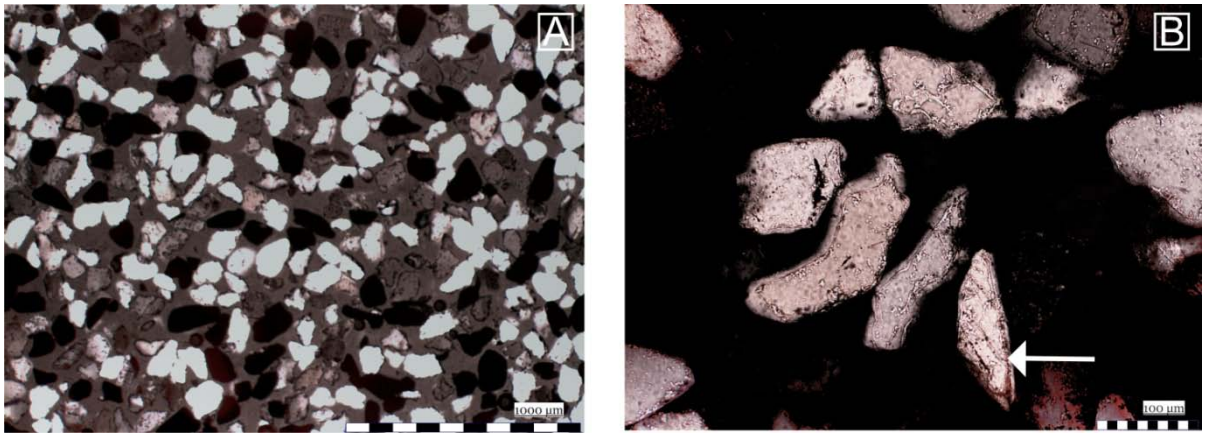

Figure 21: Optical microscopy of Ayers Rock (all photos with crossed polarizers). (A) Overview of the sample with dominant subrounded to subangular quartz grains and a significant high amount in mafic minerals. (B) Elongated to subangular quartz grains with bubbles and inclusion trails (arrow).

DEATH VALLEY - USA

Microstructural analyses of the Death Valley quartz grains show that the density of dislocations is much lower and more diffuse compared to the Ayers Rock quartz grains. The dislocations are commonly dislocation creep features which are marked by an irregular shape which appear randomly and occur mainly close to the inclusion trails. The diffraction contrast points out a few small low angle subgrain-boundaries, dominantly initiated along the pervasive inclusion trails. In addition, bubbles appear more frequently and are often accompanied by dislocations (Figure 22).

Optical microscopy analyses shows abundant angular to sub-rounded quartz grains with minor observed lattice defects such as dislocations and trails. Bubbles are common features within the Death Valley sample which occur dominantly as separate features (Figure 23 B-arrow). The content of these bubbles is unknown. Further, subgrains occur only sporadically and appear to be not as distinct as in the Ayers Rock sample.

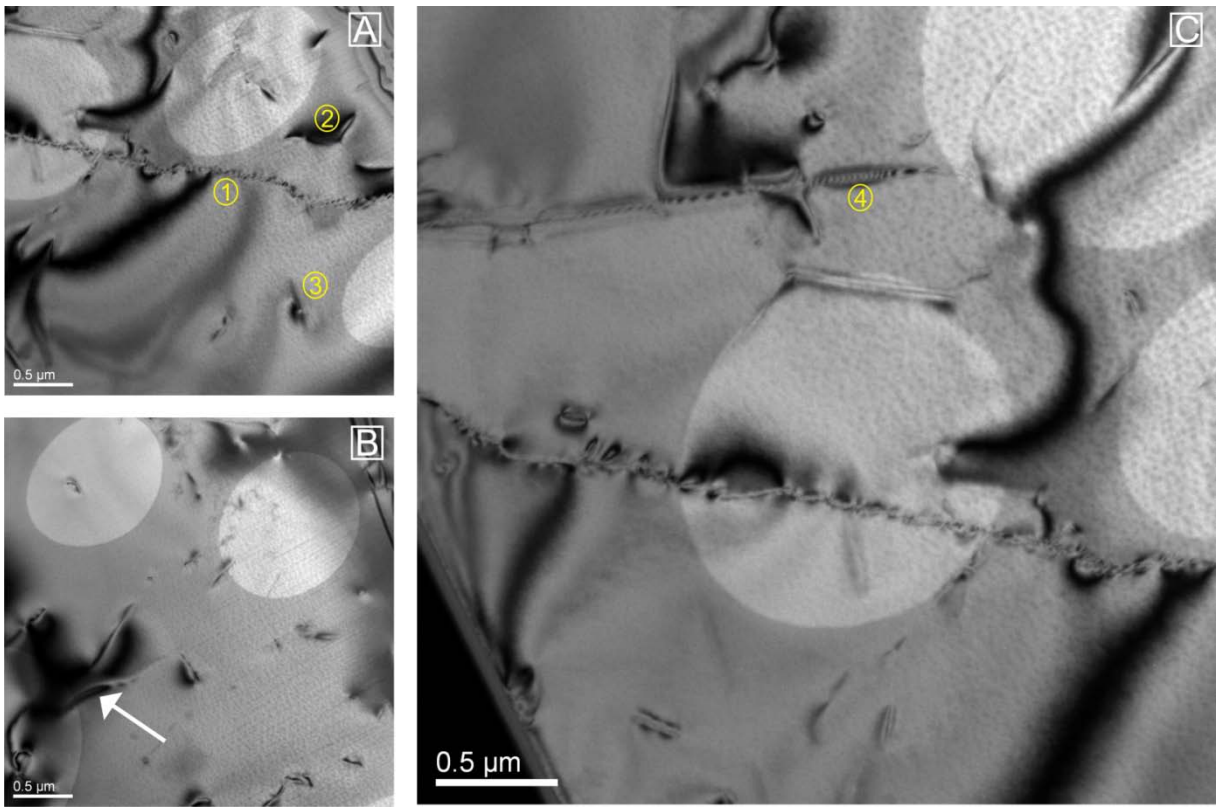

Figure 22: Microstructural analyses of Death Valley quartz grains (all bright field micrographs). (A) Subgrain boundary (1) and dislocation creep (2) with inclusion bubbles: the dislocations have been initiated along these inclusions (3). (B) Medium to low density of various dislocation features (arrow). (C) The diffraction contrast along this subgrain indicates a low angle boundary and small inclusion trails (4).

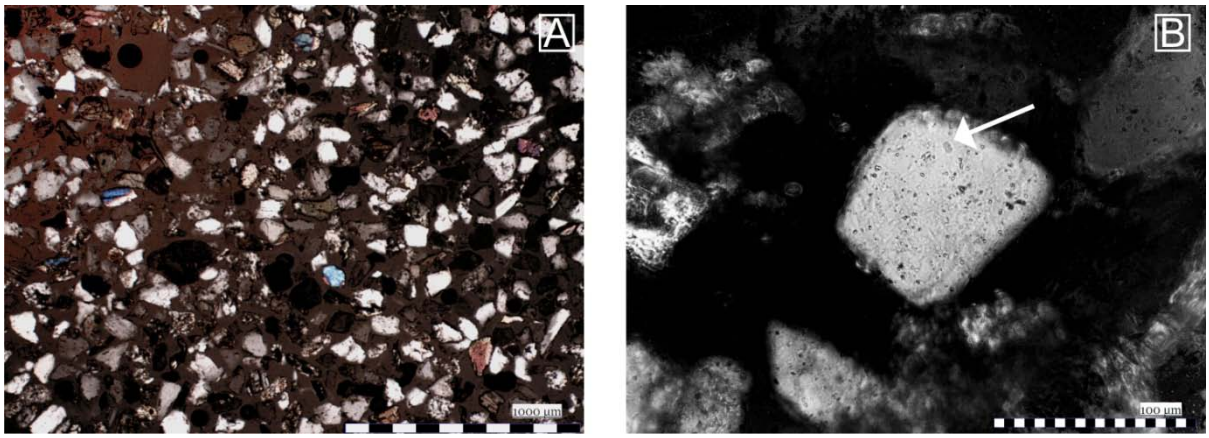

Figure 23: Optical microscopy of Death Valley (all photos with crossed polarizers). (A) Optical microscopy shows that quartz is the most abundant mineral in the Death Valley sample. Most of the quartz grains have a subangular to angular shape. (B) Showing a subangular quartz grain with some inclusions (arrow).

DUNE SANDS – NORTH ALGERIA

From *optical microscopy* observations, the quartz grains from dune sands of North Algeria are commonly subrounded to angular. Summarizing microstructural analysis, the investigated quartz grain consists of inclusion trails and bubbles (Figure 24).

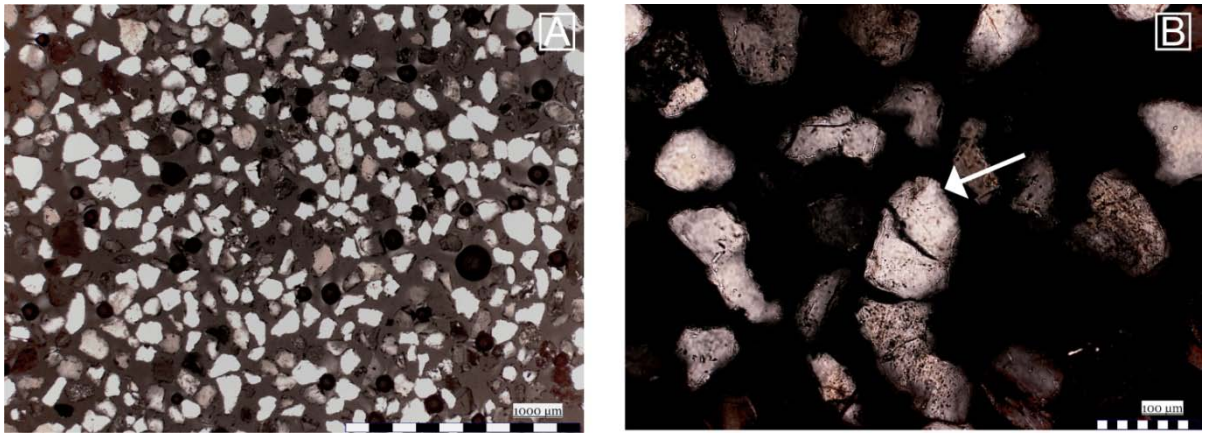

Figure 24: Optical microscopy of dune sand (North Algeria) (all photos with crossed polarizers). (A) Optical microscopy showing variations in quartz grain shape (elongated to sub-rounded). (B) Fractures (arrow) have been observed frequently along fluid inclusion trails.

The abundance of inclusion trails are higher compared to the previous described samples. Along these inclusion trails, fractures occur in many quartz grains (Figure 24 B-arrow). Moreover, undulate extinction as a hint for subgrains and subgrain boundaries are rarely seen.

LENA DELTA – RUSSIAN FEDERATION

Microstructural analyses of the Lena Delta samples show a regular occurrence of dislocations and fluid inclusions compared to Ayers Rock and Death Valley observed quartz grains. As shown in figure 25 C bubbles with different coloring appear frequently along these extensive dislocations. The dark bubbles are most likely filled with a solid content, compared to the white inclusion. The white inclusion consist either of gas or water but this could not been analyzed. The density of dislocations (Figure 25) is very high and by looking at the kind of dislocation, it is most likely that this quartz grain has experience high temperatures. The bended shape of these dislocations indicates dislocation creep which is associated with high temperature involvement. The subgrain boundary is bound by a long and pervasive inclusion trail. Along this trail bubbles and dislocations are present which makes this quartz grain probably more instable to thermal and mechanical stress (see Chapter 5).

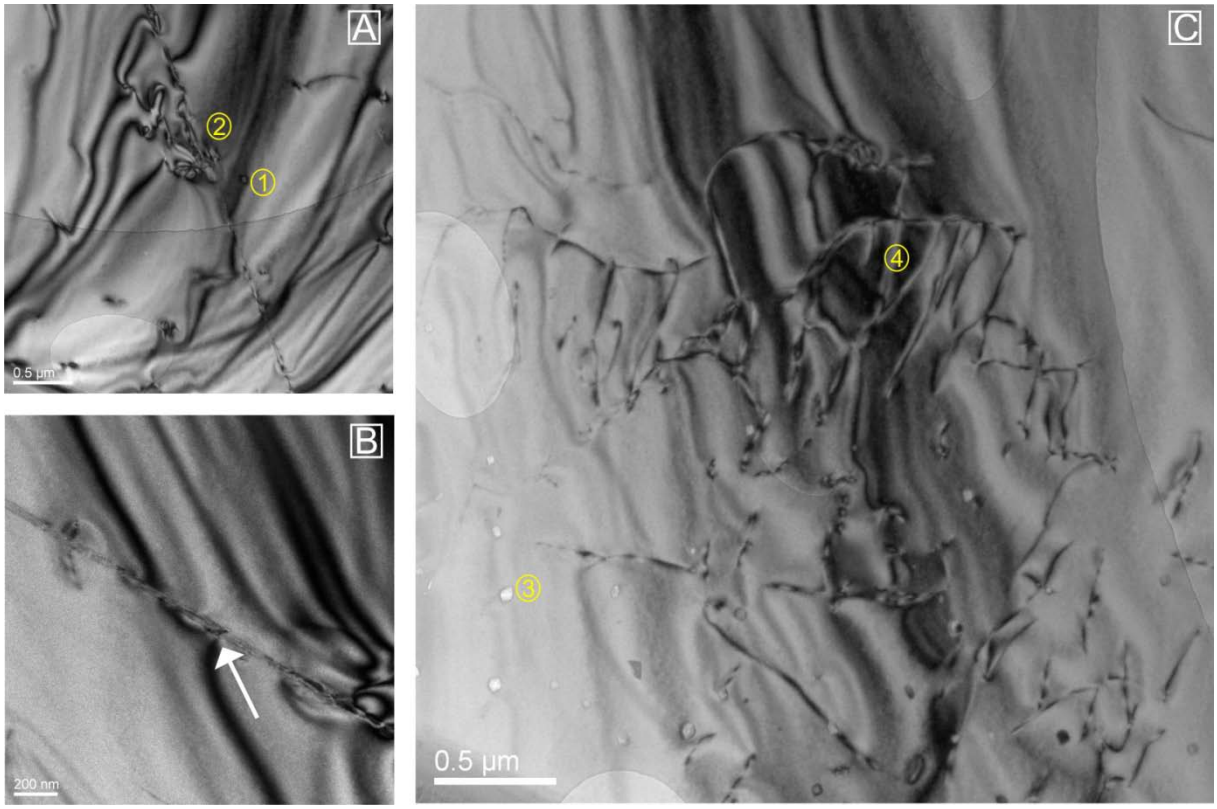

Figure 25: Microstructural analyses of Lena Delta quartz grains (all bright field micrographs). (A) The dislocation arrays extending from the (fluid) bubbles (1) which concentrate along the subgrain boundary (2) (B) The diffraction contrast indicate a low angle subgrain (arrow). (C) Enlarged view of a dense network of dislocations (4). The white and dark round spots are inclusions (3).

Optical microscopy analyses as illustrated in figure 26-center left, show wavy extinction of the quartz grain as a hint for subgrains and subgrain boundaries. In addition inclusion trails and bubbles were frequently observed in this sample (Figure 26 B-arrow).

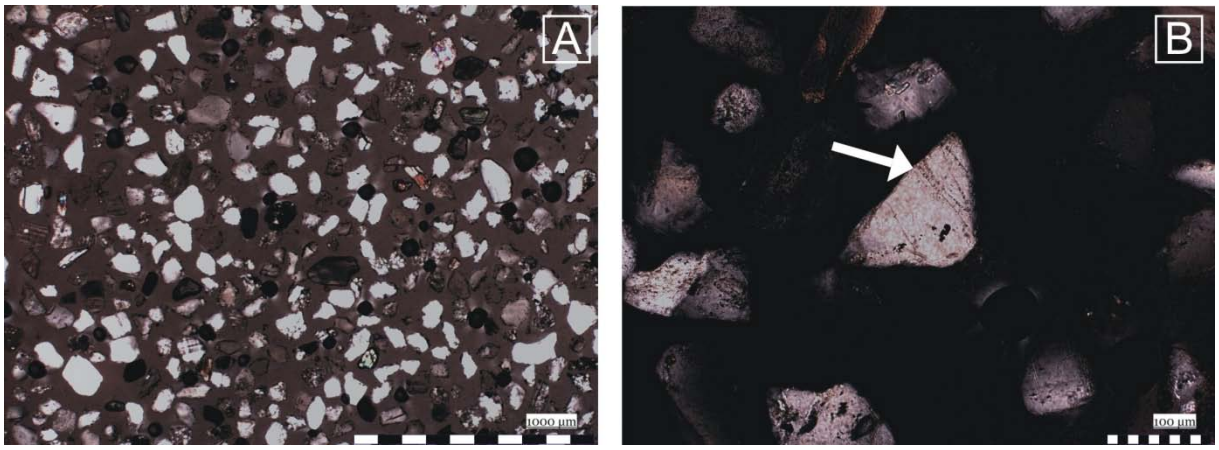

Figure 26: Optical microscopy of Lena Delta 2002 (all photos with crossed polarizers). (A) Most of the observed quartz grains are subrounded and consist commonly of inclusions (trails and bubbles) as well as subgrains. (B) The marked quartz (arrow) consists of bubbles (arrow) and inclusion trails.

The results from the optical microscopy are supporting the observations made from the TEM that the Lena Delta quartz grain samples consist of subgrains, inclusions and dislocations.

LAKE EL'GYGYTGYN – RUSSIAN FEDERATION

The following described microstructures have been performed on thin sections from whole rock samples, collected from the Lake El'gygytgyn site area (see also Figure 4).

ANDESITE-SAMPLE GS-1

Microstructural analyses of the *Andesite* quartz grain (Figure 27) show that this part of the quartz grain is marked by a continuous subgrain boundary. The development of a gap along this boundary is described as a fracture. This fracture is ideal for fluid migration during frost weathering and would therefore cause the grain to break easily along this line (see chapter 5). The dislocations are present at a medium density, intersected by the grain boundary and are only concentrated on the one side of the fracture. Comparing these observations with the previous described samples, the quartz grain lacks on dislocations and inclusion trails. The porosity displayed as white bubbles in figure 17 only rarely exist.

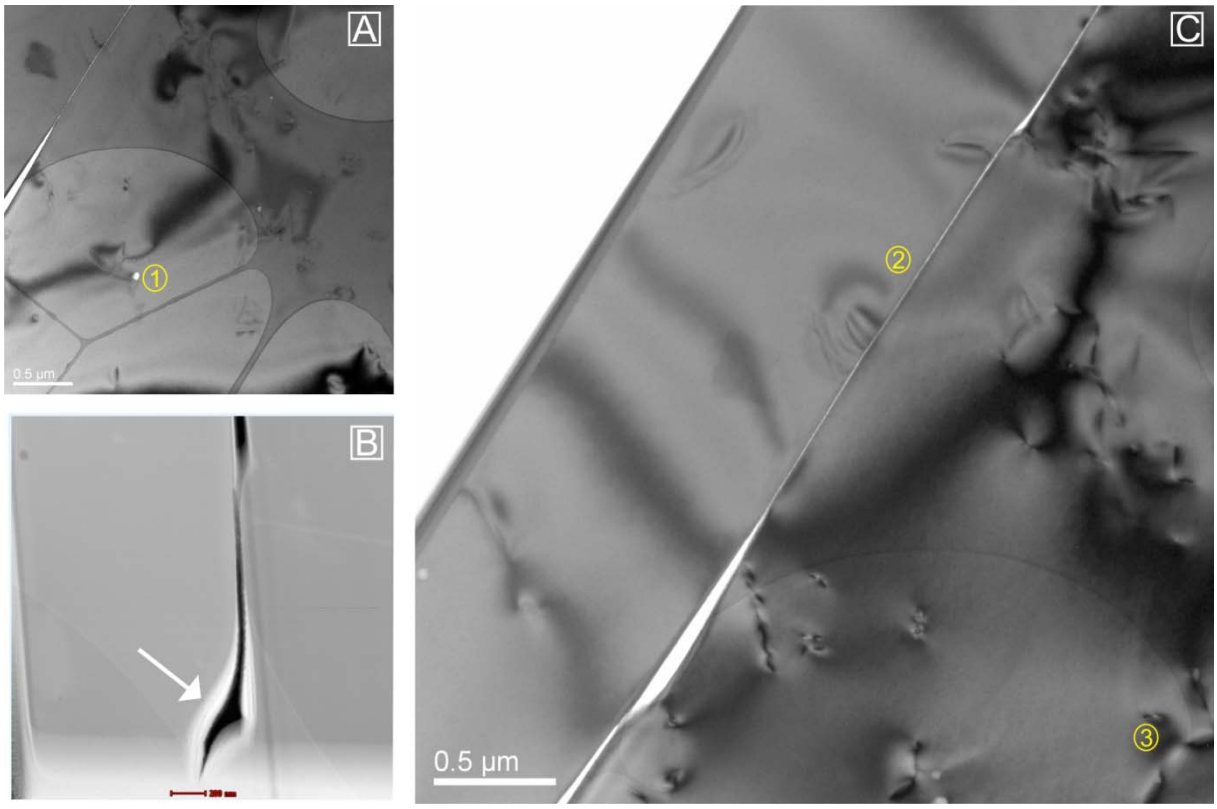

Figure 27: Microstructural analyses of Andesite contained quartz grains (GS-1) from Lake El'gygytgyn. (A) Bright field micrograph. TEM micrograph is showing a low to medium density of dislocations and inclusion bubbles (1) intersected by a pervasive subgrain boundary/fracture (upper left corner). (B) Dark field micrograph. The empty gap between the two subgrains is displayed in black (arrow). (C) Bright field micrograph. The dislocation density (3) on the right half of the subgrain boundary (2) is medium but much lower on the left part of the subgrain boundary.

Optical microscopic observations show that most of the measured grain sizes of quartz are less than 1 mm in length and width. Thin section analyses indicate a distinct increase in inclusions and subgrains (Figure 28) compared to the Lena Delta sample. As illustrated in figure 28 B, the edges along the quartz grain are highly irregular. In addition, tiny bubbles are commonly observed, mostly consisting of fluid or gas. Thin section analyses of the OM show that the Andesite consists of high amounts of secondary quartz (Figure 28 A). The primary quartz is marked as phenocryst (large minerals in a fine grained matrix) and shows strong effects of alteration as well as many inclusions (bubbles rather than trails) (Figure 28 B-arrow). Unfortunately it was not possible to identify the content of the inclusions though they mainly consist of fluids.

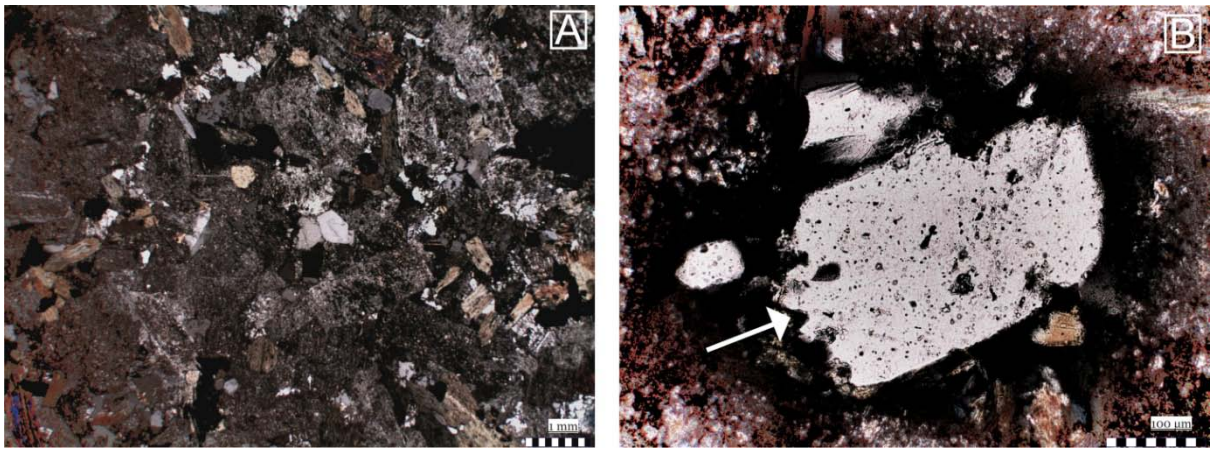

Figure 28: Optical microscopy of GS-1 Andesite (all photos with crossed polarizers). (A) Typical porphyric texture of an igneous rock. Most of the feldspar had been already silicified and altered marked by this brown to gray matrix. (B) The edges of this quartz grain (arrow) show effects of partly solution and numerous bubbles appear within the quartz grain.

Feldspar shows strong effects of silicification, marked by the transformation from commonly anhedral shapes with typical twinning lamella to a brownish fine grained matrix.

IGNIMBRITE SAMPLE GS-3

The microstructural analyses of the sample GS-3 shows the abundant occurrence of inclusion trails as well as a high porosity (voids) compared to the previously described samples from Ayers Rock and Death Valley. The inclusion trails occur as distinct and continuous features in this quartz grain sample, marked by large bubbles. These bubbles are characterized in the bright field micrograph by black subrounded shapes, which tend to initiate along discrete fractures (white linear shape). Further, this quartz grain is marked by pervasive dislocation features, which accumulate commonly along inclusion trails and subgrain boundaries. As illustrated in figure 29 D, the dislocations, which are dominantly dislocation creep features, are strong restricted on the one side of the subgrain boundary. The high density of these dislocations along this grain boundary indicates a high temperature and annealing regime.

Optical microscopy analysis confirm the observations from TEM microstructures that the quartz grains in this ignimbrite are marked by a high density of inclusion bubbles and trails (Figure 30). Therefore this TEM sample does represent microstructural features, which have been noted in most other quartz grains in GS-3.

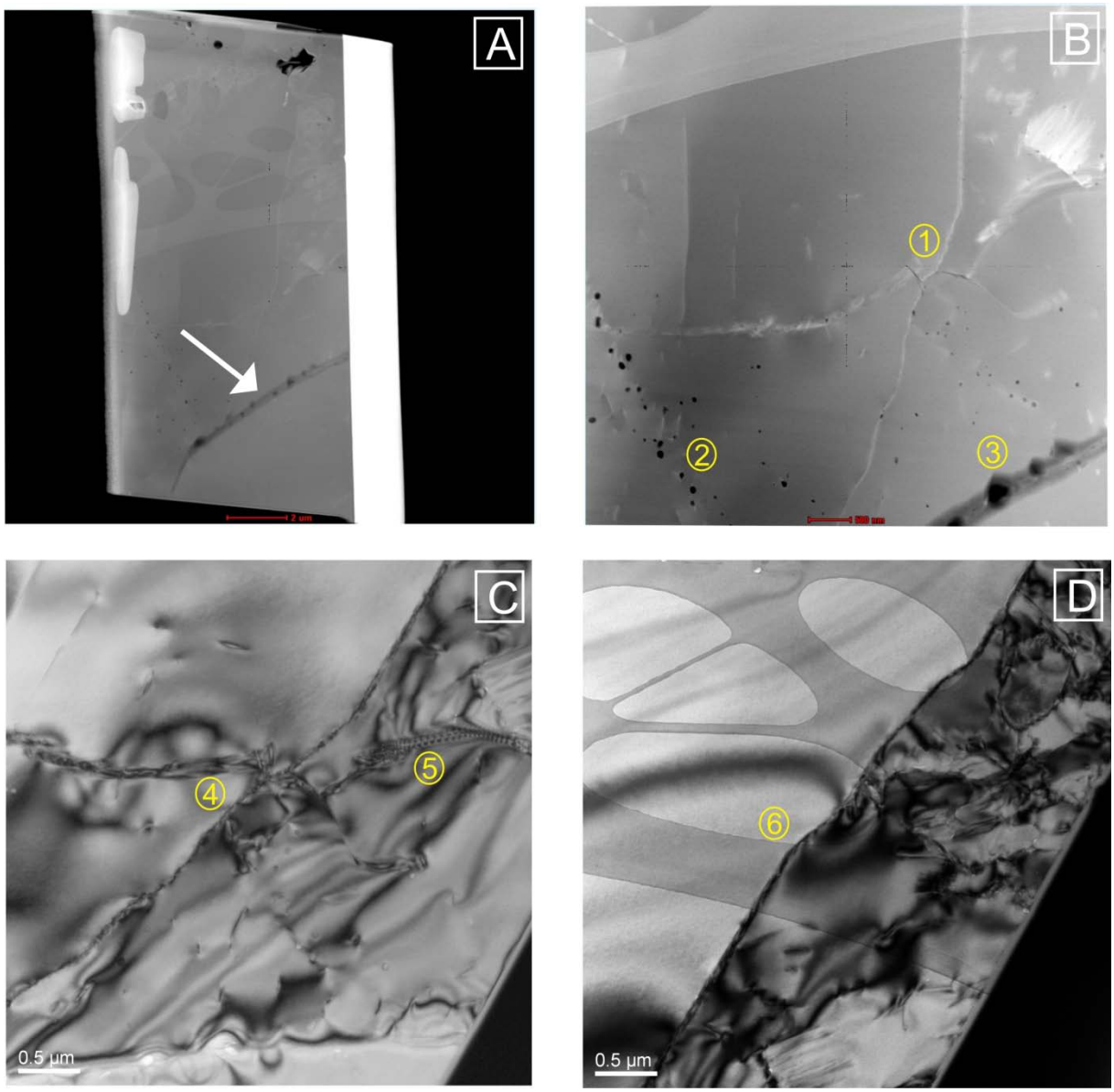

Figure 29: Microstructural analyses of Ignimbrite GS-3 contained quartz grains (GS-3). (A-D) Bright field micrographs (A) Overview of the foil sample -displaying a (fluid) inclusion trail (arrow) embedded with bubbles. The area of the arrow is enlarged in (B) showing several inclusion trails (3) and subgrain boundaries (1). It contains a high porosity displayed by dark bubbles (2). (C) The enlargement of (B-1) is showing a dense network of dislocations, bounded by several grain boundaries (4) and inclusion trails (5). (D) The displayed dislocations resulting from ductile deformation, scalloped with bowed segments in climb configuration. The dense network of dislocations is strictly limited on the right half of the subgrain boundary (6).

In addition, the ignimbrite is also dominated by secondary quartz recrystallisation (Figure 30 B-arrow), shown as fine grained quartz grains embedded with large, primary quartz grains (phenocrysts) (Figure 30 A-center). These secondary quartz grains are characterized by a commonly anhedral shape with minor to extensive fracturing features.

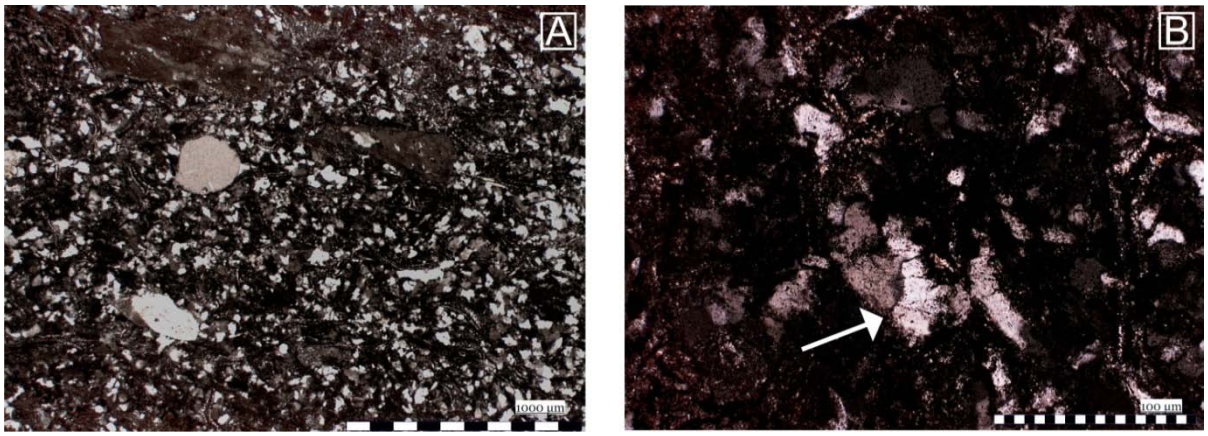

Figure 30: Optical microscopy of GS-3 Ignimbrite (all photos with crossed polarizers). (A) The optical micrograph is showing a few phenocrysts in a fine grained matrix. (B) Most of the quartz grains in the matrix are secondary quartz grains with subgrains and inclusions.

Due to the low resolution of the microscope it cannot be clearly identified if there are inclusion trails, especially along the fracture zones. The primary quartz on the contrary consists dominantly of bubbles but also of inclusion trails.

4.4 X-RAY DIFFRACTION – UNPUBLISHED DATA

As an additional method, X-ray diffraction (XRD) is used for validating and comparing the obtained SEM, TEM, OM and Laser Coulter LS 200 results. The aim of the XRD method is to *semi-quantify* changes of the quartz/feldspar ratio before and after the F/T cycles by concentrating on two main grain size fractions 32-63 µm and 63-125 µm (Schwamborn, unpublished data). This method has been introduced by Konishchev and Rogov (1993) to determine quartz enrichment in the silt fraction after F/T cycles by using the Cryogenic Weathering Index (CWI). In the framework of the cryogenic experiment, this method has been modified after Konishchev and Rogov (1993) by using grain size fractions expressed in the phi range (i.e. φ 4 and φ 5).

Before the F/T cycles, all samples from Ayers Rock, dune sands from North Algeria, Death Valley and Russian Federation (Lena Delta and Lake El'gygytgyn) are analyzed for their quartz/feldspar ratio using coarse silt and fine sand fractions (32-63 µm and 63-125 µm). Using Konishchev's formula to calculate the intensity of cryogenic weathering, the XRD data

of the two main grain size fractions have been used to estimate the CWI. Quartz enrichment in the fines is indicated when values are larger than 1. All periglacial samples from the Lena Delta and Lake El'gygytgyn show a CWI of >1. Also the Ayers Rock sample has a CWI >1, samples from the Death Valley and the Algeria dune sands show a CWI of <1.

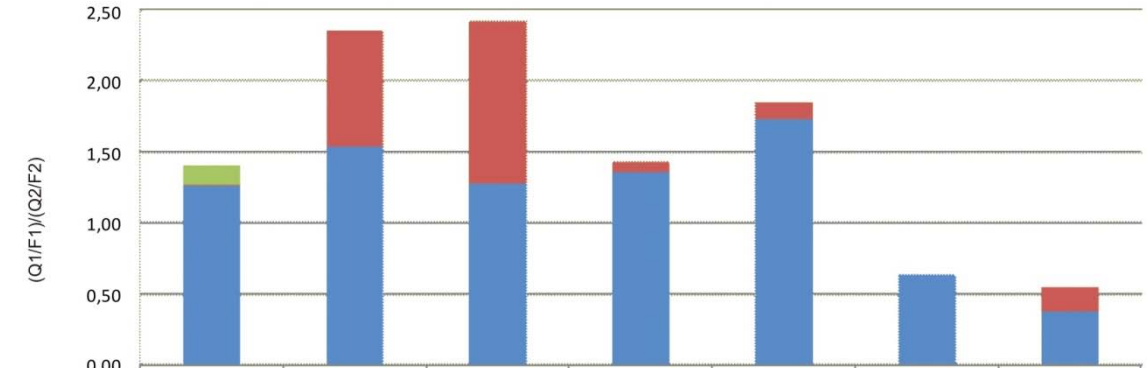

	Lake El'gygytgyn Terrace	Lena Delta 2002 ct org	Lena Delta 1998 no C org	Lake El'gygytgyn stream fill	Ayers Rock - Australia	USA-Death Valley	Dune Sands - North Algeria
Before F/T cylces	1,26	1,53	1,28	1,36	1,73	0,64	0,38
After F/T cycles	1,26	2,35	2,42	1,43	1,85	0,00	0,55
E-Lake dry beach terrace	1,40	-	-	-	-	-	-

Figure 31: Cryogenic weathering index- calculation of all measured samples before and after the F/T cycles. Based on XRD data obtained from before and after the F/T cycles.

After the F/T cycles, with the exception of Death Valley and Lake El'gygytgyn wet beach terrace, all other samples show an enrichment of quartz in the silt fraction. The variation of this increase varies between the samples but is most obvious in the Lena Delta 1998 no C_{Org} sample. For the Death Valley sample, there was not enough material in the grain size fraction 32-63 µm to conduct a XRD measurement. The Lake El'gygytgyn beach terrace (wet) sample shows no change in the CWI, which might be caused by several factors that are further discussed in chapter 5.

5 DISCUSSION

The following chapter deals with the applicability and validity of the previously described results. Furthermore, already published data from similar research topics and methods are used to compare the obtained results. The comparison of those results aims to substantiate the validity of using quartz grain textures as a proxy for cryogenic weathering.

5.1 QUARTZ GRAIN DISINTEGRATION AS A PROXY FOR CRYOGENIC WEATHERING CONDITIONS

Grain size analysis from the Ayers Rock, Lena Delta 1998 and 2002 and the Lake El'gygytgyn wet beach terrace and stream fill samples all show an increase in the grain size fraction <63 µm after F/T cycles. Further, XRD results show corresponding increases in quartz amounts in the finer fraction when comparing the initial fine fraction with the experimentally derived fine fraction. For the Lake El'gygytgyn wet beach terrace sample, the grain size measurement shows a strong increase in the silt fraction of >25 vol%. The CWI results of that particular sample do not show quartz enrichment in the silt fraction. It is speculated that unstable quartz grains may have disintegrated already in the natural permafrost environment. The random sample taken in the field may thus contain a collection of more stable quartz grains. Therefore, the results, which have been obtained from the XRD, are not absolute numbers because of the limited amount of tested samples; it might vary strongly from nature. The low increases of quartz in the XRD result the enrichment of quartz in the grain size fraction <63 µm supports Konishchev's (1982) results that quartz breaks more easily compared to feldspar under cryogenic conditions as mirrored in the F/T experimental cycling.

Schwamborn et al. (2006) investigated the sedimentary deposits of the Lake El'gygytgyn terrace samples. In a ~4.6m deep drilled core they discovered silt dominance in the upper part of the well. The silt-dominated upper part argues for extensive cold-climate weathering resulting from the breakdown of quartz (e.g. Wright et al., 1998). XRD results presented here indicate that the obtained surface material of Lake El'gygytgyn beach terrace sample has already experienced strong cryogenic weathering and therefore it already lacks fine-grained

quartz. It was not possible to generate significantly more quartz in the smaller fraction, which explains the low change of the CWI.

The investigation of the trigger mechanism for silt enrichment in glacial- and periglacial areas, quartz grain morphology in periglacial and non-periglacial areas has also been extensively analyzed and published in several papers (Pye and Sperling, 1983; Watts, 1985). Kowalkowski and Mycielska-Dowgiatto (1985) observed quartz increases with fresh conchoidal and breakage fractures in the permafrost's active layer. These observations correspond to the here presented SEM results that due to cryogenic weathering conditions, an increase in conchoidal fractures and breakage blocks are reported in most of the investigated quartz grains after the F/T cycles. Possible explanations for quartz grain disintegration are most likely due to volume extension because of the water to ice transition, as well as of mechanical and thermal stress along intragranular micro cracks. Although it does not necessarily explain why there are variations in the occurrence and intensity of fractures between the samples. An explanation might to identify the main process for quartz grain breakup several approaches are explained in the following sections.

The effect of thermal strain on quartz grains with special regard to Lake El'gygytgyn beach terrace - Indicator for cryogenic weathering conditions?

Post-experiment, a significantly more quartz is observed in the smaller grain size fraction of the Lake El'gygytgyn dry beach terrace sample, when compared to the wet beach terrace sample. Questions arise about possible causes for this difference. Studies using similar approaches have focused on thermal effects to understand the silt enrichment in periglacial regions. Pye and Sperling (1983) investigated the behavior of quartz grains under changing temperature conditions. In contrast to our experiment, they did not freeze the samples but added water to the fractionated samples and increased the temperature from +22°C to +74°C. Thus their results conclude a largely ineffective production of silt but they still produced silt in only low amounts of less than 1g. As supporting information, Kingery (1955, p.4) results shows that during heating the maximum stress is compressive on the material surface while the center is in tension. Furthermore, during cooling the maximum stress is tensile on the surface while the center undergoes compression. The results of Pye et al.

(1983) and Kingery (1955, p.4) show, regarding the Lake El'gygytgyn dry beach terrace sample that granular disintegration depend on temperature fluctuations, particularly at quartz grains under thermal strain.

Moreover, induced thermal strains can relax if temperature variations are removed depending on the grain size (Chantelois et al., 1999, p. 210). They raised the interesting observation that, as discussed by Hall (2003), achieving strain relaxation at grain scale must lead to fatigue at the grain level (Janoo et al., 1993). For the Lake El'gygytgyn dry beach terrace sample, this would suggest that the high temperature changes (shock) of up to 50°C (-20°C - +30°C) increased the internal strain. But also the volumetric expansion water as it freezes a fracturing mechanism is from equal importance for grain disintegration for the wet sample. It is to be assumed that the absence of water increased the thermal strain, since the Lake El'gygytgyn wet beach terrace sample shows lower quartz grain enrichment in the smaller fraction. Such an assumption appears important to explain the quartz enrichment in the Lake El'gygytgyn climate record during warm periods. This will be further discussed in section 5.3.

5.2 SCHEMATIC MODEL OF QUARTZ GRAIN BREAKUP BASED ON TEM & OM OBSERVATIONS

As a final approach, TEM analyses of quartz microstructures might prove useful to provide a theoretical model for quartz grain breakup. The role of inclusions in quartz in relationship with cryogenic weathering has been to date rarely investigated. Rogov (1987) pointed out that particles of quartz and other minerals can be affected by the freezing of water in gas- and/or liquid-bearing inclusions and subsequently cause the breakup of particles by the resulting volume increase when freezing occurs. Further studies (e.g. Fitz Gerald et al., 1991) investigated and discussed the effects of point defects in quartz. They conclude that fractures are important in natural fluid-rock (quartz) interaction and fractures might nucleate the dislocations necessary to initiate plastic deformation. This assumption is based on high temperature conditions (>800 °C) although it might be useful to investigate the role

of dislocations and inclusions in quartz as precursors for fractures at ambient temperatures. As already known, quartz generally contains inclusions and inclusion trails filled with e.g. salt, water or only gas. The occurrence and amount of these features vary strongly and depend on several factors such as provenance, genesis or metamorphism.

All the quartz grains presented in this study contain inclusions and/or subgrains, boundaries and dislocations, which produce lattice defects in a quartz grain on the microscopic scale. Theoretically, water-filled inclusions increase the internal strain because of volume extension as well as of thermal and mechanical stress during freezing (Figure 32). These stress factors could be initiated along those point defects but vary in their intensity by the occurrence of inclusion trails.

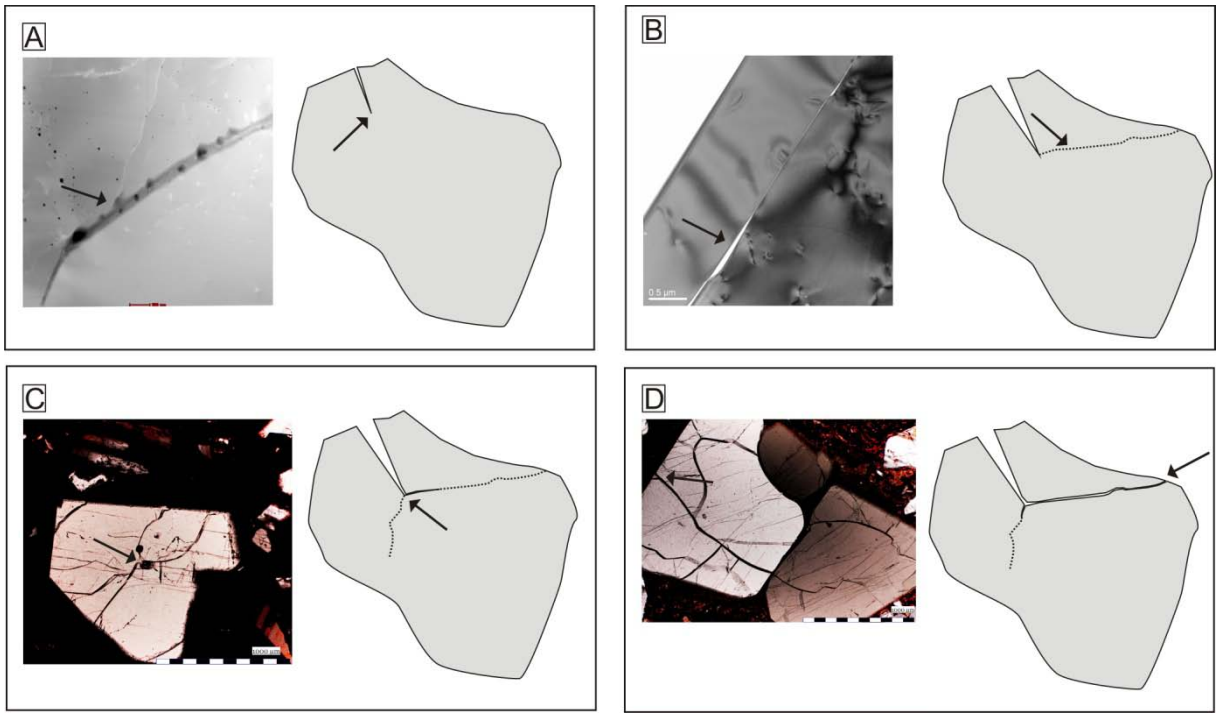

Figure 32: Schematic process of quartz grain disintegration by reviewing TEM and OM pictures of quartz grains. Presented in the diagrams are a schematic diagram (right) and an actual example (left). (A) Pre-existing fractures of inclusion trails and subgrain boundaries (TEM microphotography) lead to (B) extension of the fracture caused by migrating water (crack-see arrow) and/or thermal and mechanical stress (TEM micrograph). (C) The initiation of more fractures is supported by volume extension during thaw-freeze events (arrow in OM picture and sketch). (D) Extensive fracturing leads to breakup features of the quartz grain (arrow in OM picture and sketch).

The question is if this volume increase could overcome the internal resistance of grains to induce fracturing. This issue is not trivial as the outcome not only depends on the volume

increase of the inclusions and their density, but also on external factors such as the thickness of the water film bathing the grains and the temperature ranges used. By comparing the SEM and OM results, an increase in conchoidal fractures has been observed in all samples (see Table 4), suggests that point defects caused by the volume expansion of possible fluid-filled inclusions play an important role in inducing fractures. The TEM results of the Lena Delta samples show a high density of dislocations and porosity and at the same time an increase in conchoidal fractures and in the CWI value from 1.28 to 2.42. On the other hand, the Ayers Rock sample lacks significantly in fluid inclusions and trails, which could in turn explain the low increase of the CWI value from 1.73 to 1.85 after the experiment. The mechanisms presented here remain theoretical, but are supported by literature (Konishchev and Rogov, 1993). It has to be taken into account that morphologies of the surfaces of quartz grains and the amount of pre-existing fractures closely control the process of quartz disintegration. Further studies are needed to confirm these findings.

5.3 APPLICABILITY OF THE RESULTS IN PALEOCLIMATE RECONSTRUCTION

QUALITY OF THE OBTAINED RESULTS

In order to discuss the applicability of quartz as a proxy for paleoclimate reconstruction it is necessary to criticize the quality of the obtained results. The statistical accuracy of the SEM results is limited due to the small sample size. In spite of the reduced sampling, analyses of quartz grain morphologies identify typical shapes, e.g. aeolian-transported quartz grains. Results of grain size measurements by Laser Coulter LS 200 on two samples (Algeria, Lake El'gygytgyn beach terrace) show a hard to explain enrichment in the coarse-grained fractions. An inhomogeneous sampling might have induced this inconsistent result, which is a common problem that has to be considered. As for the TEM method, only one to two foils from quartz grains of all samples were analyzed and therefore represent only a narrow insight into the entire range of quartz microstructures. Due to time constraints in the framework of this thesis, it was not possible to investigate more quartz grains, a shortcoming partly compensated by using optical microscopy. The experiment itself helps to understand

the basic mechanisms of cryogenic weathering effects on quartz, although not reflecting the wide array of conditions found in natural environments.

USAGE OF THE RESULTS FOR PALEOCLIMATE RECONSTRUCTION

The applicability of quartz as a proxy for cryogenic weathering has been also studied by Melles et al. (2007) and Schwamborn et al. (2006, 2008). Both investigations are based on CWI calculations along two obtained cores from the Lake El'gygytgyn (Figure 33). The CWI values show in both investigations (Figure 33) variations between warm and cold periods from ~1 in warm periods and >1.7 during cold periods (particular in Melles et al. CWI values). This supports the basic conclusion that during cold periods an increase in the CWI is notable. This it does concur to the obtained CWI values of Schwamborn et al. (2006, 2008). Although questions arise regarding the high CWI values from Schwamborn et al (2006, 2008) and Melles et al. (2007) obtained in warm climate times which exceed dominantly above 1 (Figure 33, red circle).

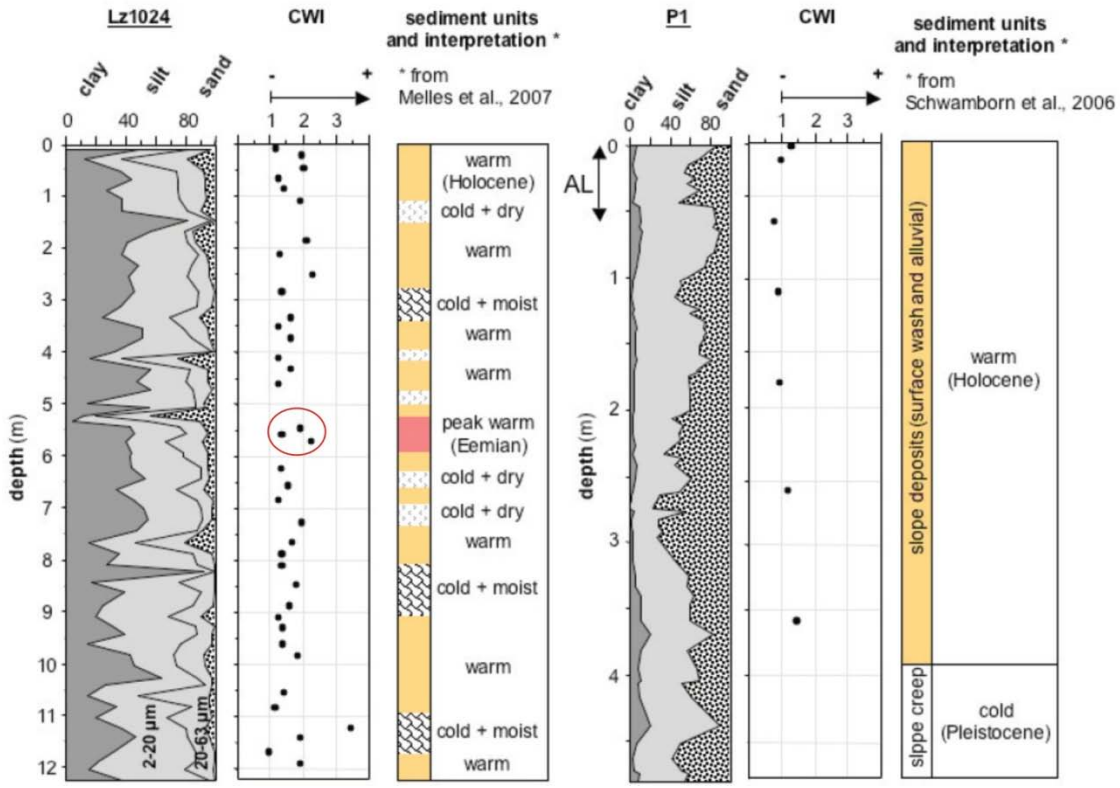

Figure 33: Values of the cryogenic weathering index (CWI) from two obtained cores from the Lake El'gygytgyn with basic sediment interpretation schemes (Schwamborn et al. 2008).

Which factor led to the increase in quartz fragmentation during a warm climate? This imply that quartz breakup properties might not rely only on temperature changes but also on observed micro fractures and state of alteration as well as on microclimate on rock surfaces and transportation/erosion processes (Schwamborn et al. 2008) as previously indicated.

The results discussed here demonstrate to some extent that Konishchev's (1982) results of stronger quartz breakup under cryogenic conditions apply according to the experimental F/T set-up. All samples have been experiencing quartz enrichment in the fines after F/T cycling but vary strong in the amount of produced silt. With special regard to the Lake El'gygytgyn samples, this area presently is marked by extensive frost weathering conditions given a mean annual air temperature of about -10°C (Brigham-Grette, et al. 2007). However, the source rock of Lake El'gygytgyn is of volcanic origin and has experienced severe alteration effects as indicated in thin section observations. The quartz grains are mainly secondary and those of primary and secondary origin have already experienced severe alteration effects, which might accelerate the quartz disintegration process. TEM images of El´gygytgyn grains show that subgrain boundaries and inclusions of gas-liquid phases may also play a role in quartz breakup dynamics. Therefore CWI calculations have to be taken with caution when taken without further insight into granular inhomogenity.
Unfortunately, in the frame work of this Master's thesis it was not possible to identify the main process which triggers the quartz fragmentation.

CWI EXTRAPOLATION ON THE BASIS OF THE OBTAINED CWI RESULTS

To investigate possible long-term behavior of quartz grains under cryogenic conditions, the CWI values of the samples from Ayers Rock, dune sands from North Algeria, Death Valley and the Russian Federation (Lena Delta and Lake El'gygytgyn) the F/T cycles are extrapolated by an assumed stable quartz decay rate (Figure 34). The results show that with a stable decay rate of quartz the most productive quartz shattering would be with the Lena Delta grains, presumably until all sand-sized quartz particles have broken apart. The Lena Delta samples are suitable for quartz grain disintegration caused by increased organic input supported by micro fractures and erosion and transportation processes. Regarding the

results from Lake El'gygytgyn, Ayers Rock, dune sands (Algeria) and Death Valley, they show strong variations in their CWI which is not surprisingly because they are based on the CWI calculations from before to after the F/T cycles.

These CWI extrapolations are based on a constant rate of sediment input by constant temperature changes using the CWI values obtained during the cryogenic experiment. These constant conditions do not occur in nature. However, estimations of quartz grain disintegration rates are difficult to calculate due to too many unknown variables and factors but still provide an important insight in possible weathering rates under laboratory conditions.

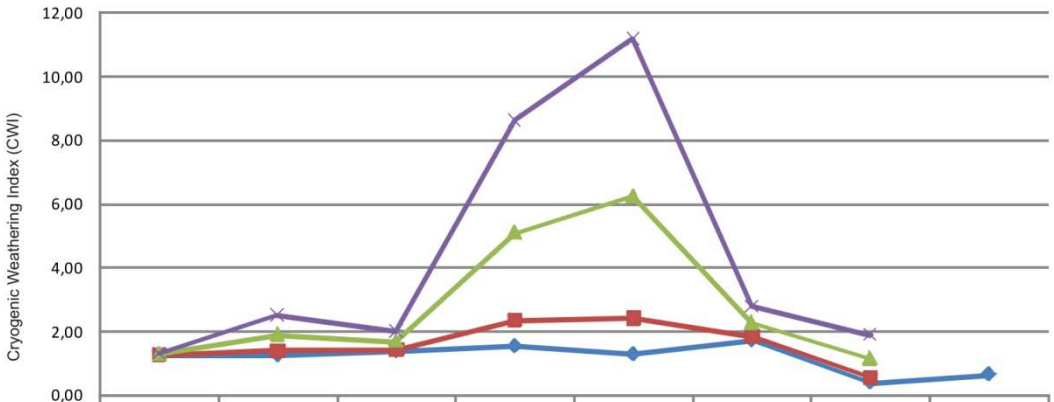

	Lake El'gygytgyn Terrace	Lake El'gygytgyn Terrace DRY	Lake El'gygytgyn stream fill	Lena Delta 2002	Lena Delta 1998	Australia	Algeria	USA-Death Valley
Before the experiment	1,26	1,26	1,36	1,53	1,28	1,73	0,38	0,64
231 cycles	1,26	1,40	1,43	2,35	2,42	1,85	0,55	-
1000 cycles	1,28	1,88	1,68	5,08	6,23	2,26	1,13	-
2000 cycles	1,31	2,50	2,00	8,62	11,18	2,79	1,89	-

CWI Extrapolation: $\frac{(CWI_2 - CWI_1)}{231} \times n$ = F/T cycles; where CWI_1 is before and CWI_2 is after the experiment

Figure 34: CWI extrapolation - an experimental approach on long-term cryogenic weathering conditions and its impact on quartz. The calculations are based on the mechanical decay rate after 231 F/T cycles.

Nevertheless, it shows that the amount of quartz fragmentation relies on several external and factors. These factors and unknown variables might be for example the amount of transported sediments and erosion rate as well as of temperature fluctuations and the presence or absence of pore water.

6 CONCLUSION

Based on my results and interpretation, Konishchev's (1982) results of preferential quartz grain disintegration under cryogenic conditions are confirmed even though the significance of the CWI appears in some cases limited. Despite a limited range of CWI values, samples from the Lake El'gygytgyn show a potential use for paleoclimate reconstruction thanks to a limited catchment area and already highly weathered rocks. Such a result disagrees with Konishchev's data namely that the higher the CWI, the greater the duration and intensity of cryogenic weathering, because the transport and intermixing of sediments somewhat interfere with the expression of cryogenic effects mainly their composition and grain size distribution.

The investigation of the reasons for easier quartz grain breakup under cryogenic condition led to several conclusions but also assumptions. Micromorphological studies of quartz grain surfaces (SEM) appear necessary to identify typical cryogenic features, e.g. cryogenic cracks. Although its validity is questionably caused by low amounts of investigated quartz grains, it shows significant changes in shape and surface features after the F/T cycles compared to before the F/T cycles. The results of the SEM investigated quartz grains shows that cryogenic weathering effects can be initiated within a freeze-thaw cycle of 231 times which correspond in most samples to the grain size measurements of the Laser Coulter. The TEM usage to analyze quartz grain lattice defects is a helpful tool to understand grain disintegration effects on a micro scale because it provided insight of microstructural features which appear in any investigated quartz grain. The optical microscopy supported these observations made from the TEM and help for a qualitative interpretation. In order to infer cryogenic weathering conditions from sedimentary archives and to identify past episodes of permafrost in Quaternary sections an approach is suggested that includes both quartz enrichment measurements in the fines and detailed SEM and TEM observations.

The reasons for quartz grain disintegration is supported by several internal (inclusion trail, subgrain boundaries, bubbles) and external (availability of water, temperature fluctuations, whole rock composition) processes but which importance and weight each process has, must be a matter of further research.

7 DANKSAGUNG

Das Thema sowie Vorbereitung und Anfertigung dieser Masterarbeit ist für mich die beste Erfahrung während meines gesamten Studiums gewesen. Daher möchte ich mich an erster Stelle bei Georg Schwamborn bedanken der mir dieses Thema angeboten hat. Er hat mich immer während dieser Zeit unterstützt und mir mit seinen zahlreichen Tipps und Anregungen, als auch mit seiner Geduld diese Masterarbeit auf Papier zu bringen, geholfen. Meinen Dank gilt auch Ekkehard Scheuber, der nicht nur durch sein umfassendes Wissen in Vulkaniten ein wichtiger Ansprechpartner war, sondern auch durch seine konstruktiven Kritiken und Ratschläge. Desweiteren möchte ich mich bei Bernhard Diekmann bedanken, der dieses Masterarbeitsthema angenommen hat.

Einen besonderen Dank gilt Quentin Scouflaire, der mir während der vielen Stunden zum Teil auch Nächte im Büro als Freund, Berater und Kritiker zur Seite stand. Ferner möchte ich mich an dieser Stelle auch bedanken bei Jan Evers, Anna Giribaldi, Ute Bastian sowie Prof. Richard Wirth und Prof. Christoph Heubeck für die freundliche Unterstützung bei der Bereitstellung und Bearbeitung der Proben. Die Freundschaft zu Audrey Bertrand, Andreas Scharf, Bianca Kallenberg und Craig Miller hat mir während dieser Zeit sehr geholfen und ist substantiell gewesen für die Erstellung dieser Masterarbeit.

Für die großartige Unterstützung während meines gesamten Studiums möchte ich mich ganz besonders bei meinen Eltern bedanken. Ohne deren Zuspruch als auch finanzielle Unterstützung wäre mein Studium nicht möglich gewesen.

8 REFERENCES

Allen T. (1997), Particle Size Measurement. *Chapman & Hall* (5th edition), Vol. 2

Asikainen C. A., Francus P., Brigham-Grette J., (2007), Sedimentology, clay mineralogy and grain-size as an indicators of 65 ka of climate changes from El'gygytgyn Crater Lake, Northeastern Siberia, *Journal of Paleolimnol*, Vol. 37, pp. 105-122

Bakker R. J., Janson J. B. H. (1994), A mechanism for preferential H2O leakage from fluid inclusions in quartz, based on TEM observations, *Contribution Mineralogy and Petrology*, Vol. 116, pp. 7-20

Belyi V. F., Belya B. V., Raikevich M. I. (1994), Pliocene deposits of upstream of the Enmyvaan River and the age of impactogenesis in the El'gygytgyn Lake Hollow. [in Russia] *Magadan*, NESRI FEB Russ Ac Sci, pp. 24

Belyi V. F., Chereshnev I. A. (eds) (1993), The nature of the El'gygytgyn Lake Hollow. [in Russia] *Magadan FEB Russ Ac Sci*, p. 250

Belyi V. F. (1982), The El'gygytgyn lake basin-meteoric crater or geological structure of the newest stage of the evolution of the Central Chukotka [in Russia] *Pacific Geology*, Vol. 5, pp. 85-91

Beuselinck L., Govers G., Poesen J., Degraer G., Froyen L. (1998), Grain-size analysis by laser diffractometry: comparision with the sieve-pipette method. *Catena*, Vol. 32, pp. 193-208

Bridgman, P. W. (1912), Water, in the liquid and five solid forms under pressure. *American Academy of Arts and Science*, Vol. 47, pp. 441-558

Brigham-Grette, J., Melles, M., Minyuk, P. and Scientific Party (2007), Overview and significance of a 250 ka paleoclimate record from El'gygytgyn Crater Lake, NE Russia. *J Paleolimnol,* Vol. 37, pp. 1–16

Chantelois A., Leger P., Tinawi R., Veileux M. (1999), Experimental and numerical predictions of critical cooling temperature for cracking propagation in concrete structures. *American Concrete Institute Structural Journal,* Vol. 96, pp. 203-211

Culver S.J., Bull P. A., Campbell S., Shakesby R. A., Whalley W. B. (1983), Environmental discrimination based on quartz grain surface textures: a statistical investigation, *Sedimentology*, Vol. 30, pp. 129-136

Douglas, G. R., McGreevy, J. P., Whalley, W. B. (1983). Rock weathering by frost shattering processes. In: Permafrost, Proceedings of the Fourth International Conference on Permafrost, 17–22

Fitz Gerald JD, Boland JN, McLaren AC, Ord A, Hobbs BE (1991) Microstructures in water-weakened single crystals of quartz. *J Geophys Res* 96(B2):2139–2155

Fliervoet, T. F., White, S. H., Drury, M. R., 1997. Evidence for Dominant Grain-Boundary Sliding Deformation in Greenschist- and Amphibolite-Grade Polymineralic Ultramylonites from the Redbank Deformed Zone, Central Australia. *J. Struct. Geol*., 19(12): 1495–1520

French H. M. (2007), The Periglacial Enviroment. *John Wiley & Sons*, Ltd (3th Edition)

Glushkova, O. Yu. (2001), Geomorphological correlation of Late Pleistocene glacial complexes of Western and Eastern Beringia. Quat Sci Rev 20:405–417

Goltrant O., Cordier P., Doukhan J.-C. (1991), Planar deformation features in shocked quartz; a transmission electron microscopy investigation*, Earth and Planetary Science Letters*, Vol. 106, pp. 103-115

Hall K. (2004), Evidence for freeze-thaw events and their implications for rock weathering in northern Canada, *Earth Surface Processes and Landforms*, Vol. 29, pp. 43-57

Hall K., M-F. Andre (2003), Rock thermal data at the grain scale: Applicability to granular disintegration in cold environments, *Earth Surface Processes and Landforms*

Hall K. (2003), Micro-transducers and high-frequency rock temperature data: changing our perspectives on rock weathering in cold regions, *Permafrost, Philips, Springman & Arenson*

Hirth G. Tullis J. (1992), Dislocation creep regimes in quartz aggregates, *Journal of Structural Geology*, Vol. 14, pp. 145-159

Janoo V., Bayer J., Walsh M. (1993), Thermal stress measurements in asphalt concrete. *Cold Regions Research and Engineering Laboratory*, Report 93-10, pp. 30

Karte, J., Liedtke, H. (1981). The theoretical and practical definition of the term 'periglacial' in its geographical and geological meaning. *Biuletyn Peryglacjalny*, Vol. 28, pp. 123–135.

Kingery W. D. (1955), Factors affecting thermal stress resistance of ceramic materials. *Journal of the American Ceramic Society*, Vol. 38, pp. 3-17

Krinsley, D.H., Doornkamp J. C. (1973), Atlas of Quartz Sand Surface Textures. 1st Edn. *Cambridge University Press, Cambridge, UK*.

Konishchev V. N., Rogov V. V. (1993), Investigation of cryogenic weathering in Europe and Northern Asia, *Permafrost and Periglacial Processes*, Vol. 4, pp. 49-64

Konishchev V. N. (1982), Characteristics of cryogenic weathering in the permafrost zone of the European USSR, *Artic and Alpine Research*, Vol. 14, Issue 3, pp. 261-265

Kowalkowski A., Mycielska-Dowgiallo E. (1985), Weathering of quartz grains in the liquefied horizon of permafrost Solonchaks in the arid steppe zone, Central Mongolia, *Catena,* Vol. 12, pp. 179-190

Layer P. W. (2000), Argon-40/argon-39 of the El'gygytgyn impact event, Chutkotka, Russia, *Meteorics & Planetary Science* Vol. 35, pp. 591-599

Lie J., Malis T., Dionne S. (2006), Recent advances in FIB-TEM specimen preparation techniques, *Material Characterization,* Vol. 54, pp. 64-70

Loizeau J. L., Arbouille D., Santiago S. (1994), Evaluation of a wide range laser diffraction grain size analyser for use with sediments. *Sedimentology*, Vol. 41, pp. 353-361

Mahaney W. C., Claridge G., Campell I. (1996), Microtextures on quartz in tills from Antarctica, *Paleogeography, Paleoclimatology, Paleoecology*, Vol. 121, pp. 89-103

Masaitis V. L. (1999), Impact structures of northeastern Eurasia: the territories of Russia and adjacent countries. Meteoritics and Planetary Science, Vol. 34, pp. 691-711

Melles M., Brigham-Grette J., Glushkova O. Y., Minyuk P. S., Nowaczek N. R., Hubberten H-W. (2007), Sedimentary geochemistry of core PG 1351 from Lake El'gygytgyn-a sensitive record of climate variability in the East Siberian Artic during the past three glacial-interglacial cycles, *Journal of Paleolimnol*, Vol. 37, pp. 89-104

Mueller S. W. (1943), Permafrost or permanently frozen ground and related engineering problems. *Special Report, Strategic Engineering Study, Intelligence Branch, Office, Chief of Engineers*, Vol. 62, pp. 136.

Niessen F., Gebhardt A. C., Kopsch C., Wagner B. (2007) Seismic investigation of the El'gygytgyn impact crater lake (Central Chukotka, NE Siberia): preliminary results. *J Paleolimnol*, Vol. 37, pp. 49-63

Nolan, M., and Brigham-Grette, J., 2007, Basic hydrology, limnology, and meteorology of modern Lake El'gygytgyn, Siberia, *Journal of Paleolimnology*. 37(1), 17-35.

Schirrmeister, L., (1995), Microfabrics, grain size distributions and grain surface textures in Late Pleistocene basin sediments of Brandenburg (NorthernBarnim). *Zeitschrift für Geomorphologie*. N. F., Supplementband 99, pp. 75–89.

Schwamborn G. Förster A., Diekmann B., Schirrmeister L., Federov G. (2009) Mid-to Late-Quaternary cryogenic weathering conditions at El'gygytgyn Crater, Northeastern Russia: Inference from mineralogical and microtextural properties of the sediment records, *Ninth International Conference on Permafrost*, pp. 1601-1606

Schwamborn G., Fedorov G., Schirrmeister L., Meyer H., Hubberten H.-W. (2008), Periglacial sediment variations controlled by late Quaternary climate and lake level change at El'gygytgyn Crater, Arctic Sibiria, *Boreas*, Vol. 37, pp. 55-65

Schwamborn, G*.,* Meyer, H*.,* Fedorov, G*.,* Schirrmeister, H., Hubberten H.-W. (2006)*,* Ground ice and slope sediments archiving Late Quaternary paleoenvironment and paleoclimate signals at the margins of Elgygytgyn Impact Crater, NE Siberia*. Quaternary Research*66*,* 259–272

Stefano C. Di, Ferro V.,Mirabile S. (2010), Comparison between grain-size analyses using laser diffraction and sedimentation methods, *Biosystems Engineering,* Vol. 106, Issue 2, pp. 205-215

Postev, N. F. *(*1977*).* Granulometric and microaggregate content of dispersed deposits of North. *Permafrost Investigation, Vol.* 16, pp.85–88 *(in Russian).*

Pye K., Sperling C. H. B. (1983), Experimental investigation of silt formation by static breakage processes: the effect of, temperature, moisture and salt on quartz dune sand and granitic regolith*, Sedimentology*, Vol. 30, pp. 49-62

Rogov, V. V. *(*1987*),* The role of gas-liquid inclusions in mechanism of cryogenic disintegration of quartz*. Vestnik of Moscow University, Geography,* No. 3, *81–85* (in Russian).

Van Hoesen J. G., Orndorff R. L. (2004), A comparative SEM study on the micromorphology of glacial and nonglacial clasts with varying age and lithology, *Canadian Journal of Earth Science*, Vol. 41, pp. 1123-1139

Vasiliyev A. A. (1994), Quantitative estimation of cryogenic weathering energy. *Permafrost and Periglacial Processes*, Vol. 5, Issue 1, pp. 67-70

Walderhaug, O. (1994), Precipitation rates for quartz cement in sandstones determined by fluid-inclusion microthermometry and temperature-history modeling, *Journal of Sedimentary Research*; Vol 64; No. 2a; pp. 324-333

Watts S. H. (1985), A scanning electron microscope study of bedrock microfractures in granites under high arctic conditions, *Earth Surface Processes and Landforms*, Vol. 10, pp. 161-172

Wilkins R. W. T., Barkas J. P. (1978), Fluid inclusions, Deformation and Recrystallization in Granite Tectonits, *Contribution to Mineralogy and Petrology*, Vol. 65, pp. 293-299

Williams P. J., Smith M. W. 1989. The Frozen Earth: Fundamentals of Geocryology. *Cambridge University Press:* Cambridge.

Wright, J. Smith B., Whalley B. (1998), Mechanism of loess-sized quartz silt production and their relative effectiveness: laboratory simulations, *Geomorphology,* Vol. 23 pp. 15-34

9 APPENDIX

This chapter includes all analytic results and calculations which are used in the framework of this Master's thesis. The appendix is subdivided into three sections:

APPENDIX 1

Overview of the statistical evaluation and calculations of shape and surface features on observed quartz grains using the *SEM* (Table B-C). The quartz grain surface and shape analyzes was performed by the below mentioned categories (Table A). These data also include additional categories which have not been further discussed in chapter Results due to its limited validity.

Table A: Shape and surface categories for quartz grain analyses

A	Large conchoidal fractures
B	Small conchoidal fractures
C	Large breakage blocks
D	Small breakage blocks
E	Arc-shaped steps
F	Random scatches and grooves
G	Oriented scatches and grooves
H	Parallel steps
I	Upturned plates
J	Micro-blocks (chemical or mechanical)
K	Roundness-rounded
L	Roundness-sub-rounded
M	Roundness-sub-angular
N	Roundness-angular
O	Precipitation features
P	Cleavage plane
Q	Solution pits and hollows
R	Subparallel linear fractures
S	Curved grooves
T	Straight grooves
U	Linear steps

Table B: SEM statistical evaluation - Before F/T cycles

Category	Algeria 1	Australia 1	USA 1	Lena Delta 1998	Lena Delta 2002	Lake El'gygytgyn beach terrace 1	Lake El'gygytgyn stream fill 1
A	1	0	5	0	10	6	3
B	0	0	4	4	10	4	4
C	2	1	6	1	11	7	6
D	3	2	8	7	10	7	5
E	6	3	8	5	9	6	5
F	5	1	3	8	10	3	3
G	6	3	10	2	9	7	5
H	1	1	5	1	7	6	4
I	3	1	3	2	0	0	0
J	2	1	2	2	0	0	0
K	0	3	0	0	0	0	0
L	9	0	1	6	0	0	0
M	3	3	4	9	5	0	1
N	0	0	6	1	6	7	6
O	10	0	2	0	1	0	0
P	6	3	11	4	10	7	7
Q	6	0	1	1	1	0	0
R	0	0	5	0	7	7	4
S	1	1	4	2	11	5	5
T	2	2	7	0	10	6	4
U	1	2	6	1	11	6	4
Summary	12	6	**11**	**16**	11	**7**	**7**

Calculation:

1%	0,12	0,06	0,11	0,16	0,11	0,07	0,07
A	8	0	45	0	91	86	43
B	0	0	36	25	91	57	57
C	17	17	55	6	100	100	86
D	25	17	73	44	83	100	71
E	50	50	73	31	82	86	71
F	42	17	27	50	91	43	43
G	50	50	91	13	82	100	71
H	8	17	45	6	64	86	57
I	25	17	27	13	0	0	0
J	17	17	18	13	0	0	0
K	0	50	0	0	0	0	0
L	75	0	9	38	0	0	0
M	25	50	36	56	45	0	14
N	0	0	55	6	55	100	86
O	83	0	18	0	9	0	0
P	50	50	100	25	91	100	100
Q	50	0	9	6	9	0	0
R	0	0	45	0	64	100	57
S	8	17	36	13	100	71	71
T	17	33	64	0	91	86	57
U	8	33	55	6	100	86	57

Table C: SEM statistical evaluation - After F/T cycles

Category	Algeria	Australia	USA	Lena Delta 1998	Lake El'gygytgyn beach terrace	Lake El'gygytgyn beach terrace DRY	Lake El'gygytgyn stream fill
A	0	1	5	0	9	11	5
B	1	1	1	0	11	11	5
C	3	2	4	0	11	12	6
D	1	5	5	0	10	13	6
E	0	2	4	0	11	12	5
F	3	0	4	0	0	0	6
G	2	4	1	0	0	0	5
H	1	0	1	0	0	0	3
I	2	0	1	0	0	0	0
J	0	0	0	0	0	0	0
K	0	2	0	0	0	0	0
L	0	0	1	0	0	0	0
M	5	0	2	3	0	1	2
N	1	3	3	0	11	12	6
O	3	0	0	3	0	3	1
P	3	1	5	3	0	0	0
Q	2	0	1	0	0	0	0
R	0	1	2	3	10	11	4
S	0	2	2	0	6	7	3
T	2	3	4	0	9	10	5
U	1	3	0	0	0	0	0
Summary	6	5	6	3	11	13	8

Calculation:

1%=	0,1	0,1	0,06	0,03	0,11	0,13	0,08
A	0,0	20,0	83,33	0,00	81,82	84,62	62,50
B	16,7	20,0	16,67	0,00	100,00	84,62	62,50
C	50,0	40,0	66,67	0,00	100,00	92,31	75,00
D	16,7	100,0	41,67	0,00	83,33	100,00	75,00
E	0,0	40,0	66,67	0,00	100,00	92,31	62,50
F	50,0	0,0	66,67	0,00	0,00	0,00	75,00
G	33,3	80,0	16,67	0,00	0,00	0,00	62,50
H	16,7	0,0	16,67	0,00	0,00	0,00	37,50
I	33,3	0,0	16,67	0,00	0,00	0,00	0,00
J	0,0	0,0	0,00	0,00	0,00	0,00	0,00
K	0,0	40,0	0,00	0,00	0,00	0,00	0,00
L	0,0	0,0	16,67	0,00	0,00	0,00	0,00
M	83,3	0,0	33,33	100,00	0,00	7,69	25,00
N	16,7	60,0	50,00	0,00	100,00	92,31	75,00
O	50,0	0,0	0,00	100,00	0,00	23,08	12,50
P	50,0	20,0	83,33	100,00	0,00	0,00	0,00
Q	33,3	0,0	16,67	0,00	0,00	0,00	0,00
R	0,0	20,0	33,33	100,00	90,91	84,62	50,00
S	0,0	40,0	33,33	0,00	54,55	53,85	37,50
T	33,3	60,0	66,67	0,00	81,82	76,92	62,50
U	16,7	60,0	0,00	0,00	0,00	0,00	0,00

APPENDIX 2: Overview of the results for grain size analyses performed on the method of laser particle sizing (Laser Coulter LS 200) (Table E-F).

Table D: Grain size measurement - Before F/T cycles

F/T cycles	Kanaldurchmesser [µm]	Algeria (vol %)	Australia-Ayers Rock (vol %)	USA-Death Valley (vol %)	Lake El'gygytgyn beach terrace (vol %)	Lake El'gygytgyn beach terrace (DRY) (vol %)	Lake El'gygytgyn stream fill (vol %)	Lena Delta 1998 no C org (vol %)	Lena Delta 2002 C org (vol %)
Before F/T cycles	0,375	0,0054	0	0	0,0051	0,0051	0	0	0,0054
	0,412	0,01	0	0	0,0097	0,0097	0	0	0,01
	0,452	0,017	0	0	0,016	0,016	0	0	0,017
	0,496	0,024	0	0	0,023	0,023	0,000076	0	0,024
	0,545	0,031	0	0	0,029	0,029	0,001	0	0,03
	0,598	0,037	0	0	0,034	0,034	0,0031	0	0,037
	0,657	0,042	0	0	0,04	0,04	0,0053	0	0,042
	0,721	0,047	0,00019	0	0,045	0,045	0,0075	0,00025	0,047
	0,791	0,051	0,0026	0	0,049	0,049	0,012	0,0033	0,052
	0,869	0,055	0,0081	0	0,053	0,053	0,019	0,01	0,056
	0,953	0,058	0,014	0	0,056	0,056	0,025	0,017	0,059
	1.047	0,059	0,019	0	0,058	0,058	0,031	0,023	0,062
	1.149	0,06	0,023	0	0,06	0,06	0,037	0,029	0,064
	1.261	0,06	0,027	0	0,06	0,06	0,041	0,034	0,064
	1.385	0,059	0,031	0	0,061	0,061	0,045	0,038	0,065
	1.520	0,057	0,034	0	0,06	0,06	0,049	0,041	0,064
	1.669	0,054	0,036	0	0,059	0,059	0,051	0,044	0,063
	1.832	0,05	0,037	0	0,058	0,058	0,053	0,045	0,061
	2.010	0,046	0,038	0	0,056	0,056	0,054	0,046	0,059
	2.207	0,042	0,038	0	0,054	0,054	0,054	0,046	0,056
	2.423	0,037	0,038	0	0,051	0,051	0,054	0,045	0,053
	2.660	0,031	0,037	0	0,049	0,049	0,053	0,043	0,051
	2.920	0,026	0,035	0	0,047	0,047	0,053	0,041	0,048
	3.206	0,021	0,033	0	0,045	0,045	0,052	0,038	0,045
	3.519	0,017	0,03	0	0,043	0,043	0,052	0,035	0,042
	3.862	0,012	0,027	0	0,042	0,042	0,052	0,032	0,04

	Kanaldurchmesser [µm]	Algeria (vol %)	Australia-Ayers Rock (vol %)	USA-Death Valley (vol %)	Lake El'gygytgyn beach terrace (vol %)	Lake El'gygytgyn beach terrace (DRY) (vol %)	Lake El'gygytgyn stream fill (vol %)	Lena Delta 1998 no C org (vol %)	Lena Delta 2002 C org (vol %)
	4.241	0,0088	0,024	0	0,042	0,042	0,052	0,029	0,038
	4.656	0,006	0,021	0	0,042	0,042	0,053	0,026	0,036
	5.111	0,0041	0,018	0	0,043	0,043	0,055	0,023	0,035
	5.611	0,0031	0,014	0	0,044	0,044	0,057	0,021	0,035
	6.158	0,0029	0,012	0	0,046	0,046	0,061	0,019	0,035
	6.761	0,0034	0,0092	0	0,049	0,049	0,065	0,018	0,035
	7.421	0,0048	0,0073	0	0,052	0,052	0,07	0,017	0,036
	8.147	0,0069	0,0061	0	0,056	0,056	0,075	0,018	0,037
	8.944	0,0096	0,0058	0	0,06	0,06	0,081	0,018	0,038
	9.819	0,013	0,0063	0,000011	0,064	0,064	0,088	0,02	0,04
	10,78	0,016	0,0079	0,00041	0,069	0,069	0,094	0,022	0,042
	11,83	0,018	0,011	0,0028	0,074	0,074	0,099	0,024	0,045
	12,99	0,02	0,014	0,0076	0,079	0,079	0,1	0,026	0,048
	14,26	0,02	0,018	0,014	0,085	0,085	0,11	0,028	0,051
	15,65	0,019	0,023	0,022	0,093	0,093	0,12	0,031	0,055
	17,18	0,017	0,027	0,03	0,11	0,11	0,12	0,036	0,06
	18,86	0,016	0,032	0,036	0,12	0,12	0,13	0,041	0,065
	20,7	0,019	0,035	0,038	0,15	0,15	0,15	0,048	0,075
	22,73	0,03	0,038	0,037	0,18	0,18	0,17	0,057	0,09
	24,95	0,054	0,043	0,035	0,22	0,22	0,2	0,066	0,12
	27,38	0,093	0,052	0,039	0,28	0,28	0,23	0,079	0,16
	30,07	0,14	0,071	0,058	0,34	0,34	0,27	0,099	0,21
	33	0,19	0,1	0,098	0,42	0,42	0,32	0,13	0,27
	36,24	0,22	0,15	0,16	0,52	0,52	0,39	0,19	0,33
	39,77	0,23	0,21	0,23	0,67	0,67	0,48	0,27	0,39
	43,66	0,27	0,27	0,29	0,9	0,9	0,63	0,38	0,47
	47,93	0,44	0,32	0,33	1,3	1,3	0,91	0,52	0,68
	52,63	0,95	0,4	0,42	1,96	1,96	1,4	0,7	1,18
	57,77	2,05	0,6	0,67	2,96	2,96	2,2	1,01	2,16
	63,41	3,9	1,08	1,29	4,33	4,33	3,38	1,57	3,76
	69,62	6,42	2,08	2,53	5,98	5,98	4,91	2,59	5,9

	Kanaldurchmesser [µm]	Algeria (vol %)	Australia-Ayers Rock (vol %)	USA-Death Valley (vol %)	Lake El'gygytgyn beach terrace (vol %)	Lake El'gygytgyn beach terrace (DRY) (vol %)	Lake El'gygytgyn stream fill (vol %)	Lena Delta 1998 no C org (vol %)	Lena Delta 2002 C org (vol %)
	76,43	9,22	3,77	4,54	7,74	7,74	6,66	4,26	8,22
	83,9	11,7	6,17	7,21	9,33	9,33	8,42	6,59	10,2
	92,09	13,1	8,97	10,1	10,5	10,5	9,92	9,31	11,5
	101,1	13,2	11,6	12,5	10,9	10,9	10,8	11,8	11,7
	111	11,9	13,3	13,8	10,4	10,4	10,9	13,2	10,9
	121,8	9,58	13,6	13,5	9,05	9,05	10	13	9,26
	133,7	6,79	12,3	11,8	7,07	7,07	8,23	11,3	7,18
	146,8	4,16	9,83	9,01	4,89	4,89	6,02	8,43	5,05
	161,2	2,11	6,85	5,99	2,97	2,97	3,91	5,42	3,2
	176,8	0,8	4,05	3,31	1,64	1,64	2,35	2,97	1,8
	194,2	0,21	1,98	1,44	0,95	0,95	1,49	1,46	0,91
	213,2	0,072	0,7	0,38	0,72	0,72	1,14	0,79	0,47
	234,1	0,13	0,23	0,026	0,67	0,67	1,02	0,62	0,34
	256,8	0,26	0,21	0	0,52	0,52	0,81	0,63	0,35
	282,1	0,25	0,17	0	0,2	0,2	0,36	0,57	0,39
	309,6	0,14	0,02	0	0,017	0,017	0,054	0,44	0,37
	339,8	0,067	0	0	0,000029	0,000029	0,0014	0,31	0,24
	373,1	0,013	0	0	0	0	0	0,16	0,066
	409,6	0,00049	0	0	0	0	0	0,035	0,004
	449,7	0	0	0	0	0	0	0,0017	0

Table E: Grain size measurement - After F/T cycles

F/T cycles	Kanaldurchmesser [µm]	Algeria (vol %)	Australia-Ayers Rock (vol %)	USA-Death Valley (vol %)	Lake El'gygytgyn beach terrace (vol %)	Lake El'gygytgyn beach terrace (DRY) (vol %)	Lake El'gygytgyn stream fill (vol %)	Lena Delta 1998 no C org (vol %)	Lena Delta 2002 C org (vol %)
After F/T cycles	0,375	0	0,011	0	0,029	0,0045	0,012	0	0,0076
	0,412	0	0,02	0	0,052	0,0087	0,023	0	0,014
	0,452	0	0,034	0	0,076	0,015	0,038	0	0,024
	0,496	0,0003	0,047	0	0,11	0,02	0,052	0,00027	0,033
	0,545	0,004	0,059	0	0,14	0,026	0,065	0,0036	0,042
	0,598	0,012	0,07	0	0,16	0,031	0,077	0,011	0,049
	0,657	0,021	0,08	0	0,19	0,036	0,088	0,019	0,056
	0,721	0,029	0,088	0,00015	0,21	0,04	0,097	0,026	0,062
	0,791	0,036	0,095	0,002	0,23	0,044	0,1	0,032	0,066
	0,869	0,043	0,1	0,0063	0,25	0,047	0,11	0,038	0,07
	0,953	0,048	0,1	0,01	0,27	0,05	0,11	0,044	0,072
	1.047	0,053	0,1	0,014	0,28	0,052	0,11	0,048	0,073
	1.149	0,056	0,1	0,018	0,3	0,054	0,12	0,052	0,072
	1.261	0,059	0,1	0,021	0,31	0,054	0,12	0,055	0,071
	1.385	0,06	0,1	0,024	0,32	0,055	0,12	0,058	0,069
	1.520	0,06	0,097	0,027	0,33	0,054	0,12	0,059	0,067
	1.669	0,059	0,093	0,029	0,34	0,053	0,12	0,06	0,065
	1.832	0,057	0,089	0,031	0,35	0,052	0,12	0,06	0,063
	2.010	0,054	0,086	0,032	0,36	0,05	0,12	0,059	0,062
	2.207	0,05	0,083	0,033	0,38	0,048	0,13	0,058	0,062
	2.423	0,045	0,082	0,033	0,39	0,046	0,14	0,056	0,062
	2.660	0,04	0,082	0,033	0,41	0,043	0,15	0,054	0,064
	2.920	0,035	0,083	0,032	0,42	0,041	0,17	0,052	0,068
	3.206	0,029	0,085	0,031	0,44	0,039	0,19	0,05	0,072
	3.519	0,024	0,089	0,03	0,46	0,037	0,21	0,049	0,078
	3.862	0,019	0,094	0,028	0,48	0,036	0,23	0,047	0,085
	4.241	0,014	0,1	0,026	0,5	0,035	0,26	0,046	0,092
	4.656	0,01	0,11	0,024	0,51	0,035	0,28	0,045	0,1
	5.111	0,0073	0,11	0,022	0,53	0,035	0,3	0,045	0,11

	Kanaldurchmesser [µm]	Algeria (vol %)	Australia-Ayers Rock (vol %)	USA-Death Valley (vol %)	Lake El'gygytgyn beach terrace (vol %)	Lake El'gygytgyn beach terrace (DRY) (vol %)	Lake El'gygytgyn stream fill (vol %)	Lena Delta 1998 no C org (vol %)	Lena Delta 2002 C org (vol %)
	5.611	0,0053	0,12	0,021	0,54	0,036	0,32	0,046	0,12
	6.158	0,0043	0,12	0,019	0,56	0,038	0,34	0,047	0,12
	6.761	0,0042	0,13	0,017	0,57	0,04	0,35	0,048	0,13
	7.421	0,005	0,14	0,016	0,57	0,043	0,37	0,05	0,14
	8.147	0,0066	0,14	0,015	0,58	0,046	0,39	0,052	0,15
	8.944	0,0089	0,15	0,014	0,58	0,05	0,4	0,055	0,17
	9.819	0,012	0,16	0,015	0,58	0,054	0,42	0,056	0,18
	10,78	0,014	0,16	0,016	0,58	0,058	0,44	0,058	0,2
	11,83	0,016	0,17	0,017	0,58	0,062	0,45	0,059	0,22
	12,99	0,017	0,18	0,019	0,58	0,066	0,47	0,061	0,25
	14,26	0,018	0,2	0,022	0,58	0,071	0,48	0,063	0,27
	15,65	0,017	0,21	0,024	0,6	0,077	0,5	0,066	0,29
	17,18	0,016	0,23	0,026	0,62	0,086	0,51	0,073	0,32
	18,86	0,015	0,26	0,026	0,66	0,097	0,53	0,081	0,36
	20,7	0,016	0,29	0,024	0,73	0,11	0,55	0,091	0,41
	22,73	0,021	0,33	0,023	0,82	0,13	0,57	0,1	0,48
	24,95	0,031	0,37	0,023	0,93	0,16	0,59	0,11	0,56
	27,38	0,051	0,41	0,029	1,05	0,2	0,6	0,11	0,66
	30,07	0,081	0,46	0,047	1,18	0,26	0,62	0,12	0,79
	33	0,12	0,53	0,079	1,31	0,32	0,66	0,14	0,96
	36,24	0,15	0,62	0,12	1,45	0,41	0,72	0,18	1,19
	39,77	0,16	0,73	0,16	1,64	0,53	0,81	0,24	1,47
	43,66	0,17	0,87	0,18	1,93	0,72	0,94	0,31	1,78
	47,93	0,24	1,06	0,19	2,35	1,05	1,17	0,39	2,15
	52,63	0,49	1,38	0,23	2,98	1,59	1,57	0,47	2,65
	57,77	1,14	1,96	0,45	3,81	2,42	2,24	0,63	3,41
	63,41	2,43	2,98	1,06	4,82	3,59	3,23	1,03	4,48
	69,62	4,49	4,56	2,35	5,89	5,07	4,52	1,91	5,81
	76,43	7,19	6,69	4,47	6,87	6,74	5,98	3,55	7,15
	83,9	10,1	9,08	7,28	7,57	8,39	7,46	6,09	8,24
	92,09	12,7	11,2	10,3	7,85	9,77	8,76	9,24	8,88

	Kanaldurchmesser [µm]	Algeria (vol %)	Australia-Ayers Rock (vol %)	USA-Death Valley (vol %)	Lake El'gygytgyn beach terrace (vol %)	Lake El'gygytgyn beach terrace (DRY) (vol %)	Lake El'gygytgyn stream fill (vol %)	Lena Delta 1998 no C org (vol %)	Lena Delta 2002 C org (vol %)
	101,1	14,1	12,5	12,9	7,63	10,6	9,64	12,3	8,99
	111	13,9	12,3	14,2	6,9	10,5	9,83	14,3	8,53
	121,8	12,1	10,7	13,9	5,74	9,57	9,16	14,6	7,53
	133,7	9,2	8,06	12	4,31	7,83	7,65	12,8	6,15
	146,8	5,93	5,05	9,03	2,84	5,69	5,62	9,63	4,59
	161,2	3,05	2,4	5,84	1,56	3,56	3,54	6	3,07
	176,8	0,98	0,62	3,05	0,65	1,8	1,84	2,82	1,77
	194,2	0,12	0,04	1,12	0,18	0,67	0,78	0,76	0,88
	213,2	0,003	0	0,22	0,026	0,17	0,36	0,07	0,5
	234,1	0	0	0,011	0,0012	0,079	0,29	0,0013	0,44
	256,8	0	0	0	0	0,16	0,31	0	0,49
	282,1	0	0	0	0	0,12	0,19	0	0,52
	309,6	0	0	0	0	0,013	0,056	0	0,46
	339,8	0	0	0	0	0	0,0097	0	0,2
	373,1	0	0	0	0	0	0,00038	0	0,018
	409,6	0	0	0	0	0	0	0	0
	449,7	0	0	0	0	0	0	0	0

APPENDIX 3: Overview of XRD data collection and calculation kindly provided by Dr. Georg Schwamborn (unpublished data) (Table F-H). The original quartz and feldspar values are displayed in dÅ which describes the covered area within the mineral specific peek. One sample was measured again due to unusual strong variation in Q/F ratio.

Abbreviations: - Q1 = Quartz before F/T cycles

- F1 = Feldspar before F/T cycles
- Q2 = Quartz after F/T cycles
- F2 = Feldspar after F/T cycles
-

Table F: XRD data of quartz/feldspar ratio - Before F/T cycles

Location			Q1	F1	Q/F ratio
Before F/T cycles	**Grain size**	**Comments**	**Qrz dÅ 4,26**	**Fsp dÅ 3,24+3,18**	**(Q1/F1)**
Lake El'gygytgyn Terrace (32-63 µm) 1	32-63 µm		1429	5835	0,24
Lena Delta 2002 (32-63 µm) 1	32-63 µm		1526	6387	0,24
Lena Delta 1998 (32-63 µm) 1	32-63 µm		8567	28837	0,30
Lake El'gygytgyn stream fill (32-63 µm) 1	32-63 µm		1342	3607	0,37
Australia (32-63 µm) 1	32-63 µm		13585	5907	2,30
USA-Death Valley (32-63 µm) 1	32-63 µm		762	2580	0,30
Algeria (32-63 µm) 1	32-63 µm		14775	11539	1,28
Lake El'gygytgyn Terrace (32-63 µm) 2	32-63 µm	repeated measurement	1217	3843	0,32
Lake El'gygytgyn Terrace DRY (32-63 µm) 2	32-63 µm		1314	6623	0,20
Lena Delta 2002 (32-63 µm) 2	32-63 µm		1172	4137	0,28
Lena Delta 1998 (32-63 µm) 2	32-63 µm		955	2616	0,37
Lake El'gygytgyn stream fill (32-63 µm) 2	32-63 µm		1233	4516	0,27
Australia (32-63 µm) 2	32-63 µm		11776	3884	3,03
USA-Death Valley (32-63 µm) 2	32-63 µm		no data	no data	0
Algeria (32-63 µm) 2	32-63 µm		2855	1064	2,68

Table G: XRD data of quartz/feldspar ratio with additional CWI calculation - After F/T cycles

Location			Q2	F2	(Q2/F2)	(Q1/F1)/(Q2/F2)
After F/T cycles	**Grain size**	**Comments**	**Qrz dÅ 4,26**	**Fsp dÅ 3,24+3,18**		
Lake El'gygytgyn Terrace (63-125 µm) 1	63-125 µm		1577	8109	0,19	1,26
Lena Delta 2002 (63-125 µm) 1	63-125 µm		1275	8191	0,16	1,53
Lena Delta 1998 (63-125 µm) 1	63-125 µm		8983	38593	0,23	1,28
Lake El'gygytgyn stream fill (63-125 µm) 1	63-125 µm		1343	4892	0,27	1,36
Australia (63-125 µm) 1	63-125 µm		13019	9781	1,33	1,73
USA-Death Valley (63-125 µm) 1	63-125 µm		1065	2293	0,46	0,64
Algeria (63-125 µm) 1	63-125 µm		16167	4739	3,41	0,38
Lake El'gygytgyn Terrace (63-125 µm) 2	63-125 µm	repeated measurement	1295	5172	0,25	1,26
Lake El'gygytgyn Terrace DRY (63-125 µm) 2	63-125 µm		1370	9687	0,14	1,40
Lena Delta 2002 (63-125 µm) 2	63-125 µm		1331	11054	0,12	2,35
Lena Delta 1998 (63-125 µm) 2	63-125 µm		1850	12265	0,15	2,42
Lake El'gygytgyn stream fill (63-125 µm) 2	63-125 µm		1288	6747	0,19	1,43
Australia (63-125 µm) 2	63-125 µm		2401	1465	1,64	1,85
USA-Death Valley (63-125 µm) 2	63-125 µm		895	7089	0,13	0,00
Algeria (63-125 µm) 2	63-125 µm		3755	770	4,88	0,55

Table H: CWI extrapolation based on collected XRD data (see Table F-G)

Location	Before the F/T cycles	231 F/T cycles	1000 F/T cycles	2000 F/T cycles
Lake El'gygytgyn Terrace	1,26	1,26	1,28	1,31
Lake El'gygytgyn Terrace DRY	1,26	1,40	1,88	2,50
Lake El'gygytgyn stream fill	1,36	1,43	1,68	2,00
Lena Delta 2002	1,53	2,35	5,08	8,62
Lena Delta 1998	1,28	2,42	6,23	11,18
Australia	1,73	1,85	2,26	2,79
Algeria	0,38	0,55	1,13	1,89
USA-Death Valley	0,64	0,00	0,00	0,00